AL/CF-TR-1995-0054

REMOVING IMPULSE NOISE FROM HUMAN HEAD SCAN DATA (U)

Joseph H. Nurre

DEPARTMENT OF ELECTRICAL & COMPUTER ENGINEERING
OHIO UNIVERSITY
ATHENS, OHIO 45701

Jennifer J. Whitestone
Jeffrey W. Hoffmeister

CREW SYSTEMS DIRECTORATE
HUMAN ENGINEERING DIVISION
WRIGHT-PATTERSON AIR FORCE BASE, OHIO 45433-7022

Dennis B. Burnsides

SYTRONICS, INC.
3 DAYTON-XENIA ROAD; BLDG 1
DAYTON, OHIO 45432-1949

MARCH 1995

INTERIM REPORT FOR THE PERIOD SEPTEMBER 1993 - JUNE 1994

AIR FORCE MATERIEL COMMAND
WRIGHT-PATTERSON AIR FORCE BASE, OHIO 45433-6573

NOTICES

When US Government drawings, specifications, or other data are used for any purpose other than a definitely related Government procurement operation, the Government thereby incurs no responsibility nor any obligation whatsoever, and the fact that the Government may have formulated, furnished, or in any way supplied the said drawings, specifications, or other data, is not to be regarded by implication or otherwise, as in any manner licensing the holder or any other person or corporation, or conveying any rights or permission to manufacture, use, or sell any patented invention that may in any way be related thereto.

Please do not request copies of this report from the Armstrong Laboratory. Additional copies may be purchased from:

National Technical Information Service
5285 Port Royal Road
Springfield, Virginia 22161

Federal Government agencies and their contractors registered with the Defense Technical Information Center should direct requests for copies of this report to:

Defense Technical Information Center
Cameron Station
Alexandria, Virginia 22314

TECHNICAL REVIEW AND APPROVAL

AL/CF-TR-1995-0054

This report has been reviewed by the Office of Public Affairs (PA) and is releasable to the National Technical Information Service (NTIS). At NTIS, it will be available to the general public, including foreign nations.

This technical report has been reviewed and is approved for publication.

FOR THE COMMANDER

KENNETH R. BOFF, Chief
Human Engineering Division
Armstrong Laboratory

REPORT DOCUMENTATION PAGE

Form Approved
OMB No. 0704-0188

1. AGENCY USE ONLY *(Leave blank)*	2. REPORT DATE	3. REPORT TYPE AND DATES COVERED
		INTERIM - SEP 1993 - JUN 1994

4. TITLE AND SUBTITLE

Removing Impulse Noise from Human Head Scan Data

5. FUNDING NUMBERS

C-F49670-93-C-0076
PR-7184
TA-08
WU-50

6. AUTHOR(S)

Joseph H. Nurre; Jennifer J. Whitestone; Jeffrey W. Hoffmeister; Dennis B. Burnsides

7. PERFORMING ORGANIZATION NAME(S) AND ADDRESS(ES)

Department of Electrical and Computer Engineering
Ohio University
Athens OH 45701

8. PERFORMING ORGANIZATION REPORT NUMBER

9. SPONSORING/MONITORING AGENCY NAME(S) AND ADDRESS(ES)

Armstrong Laboratory, Crew Systems Directorate
Human Engineering Division
Human Systems Center
Air Force Materiel Command
Wright-Patterson AFB OH 45433-7022

10. SPONSORING/MONITORING AGENCY REPORT NUMBER

11. SUPPLEMENTARY NOTES

12a. DISTRIBUTION/AVAILABILITY STATEMENT

Approved for public release; distribution is unlimited

12b. DISTRIBUTION CODE

13. ABSTRACT *(Maximum 200 words)*

This report presents a mathematical morphological filtering technique to eliminate impulse noise from human head surface data generated by laser surface scanning technologies. In the area of image processing, mathematical morphology refers to a branch of nonlinear filters which use geometric form and structure to alter a signal. Several structuring elements were investigated with a spherical structuring element being selected as the best candidate. A spherical element is the ideal shape since protruding shapes like spikes on the human head are best removed using a structuring element that has an omni-directional behavior. A spherical structuring element having a radius of 3.0mm to 3.5mm represented the best trade-off between identification of impulse noise and loss of good data points.

14. SUBJECT TERMS

Morphology	Surface Scanning	Human Head Topography
Impulse Noise	Erosion	Data Smoothing
Structuring Element	Dilation	Image Visualization

15. NUMBER OF PAGES

73

16. PRICE CODE

17. SECURITY CLASSIFICATION OF REPORT	18. SECURITY CLASSIFICATION OF THIS PAGE	19. SECURITY CLASSIFICATION OF ABSTRACT	20. LIMITATION OF ABSTRACT
UNCLASSIFIED	UNCLASSIFIED	UNCLASSIFIED	UL

THIS PAGE INTENTIONALLY LEFT BLANK

PREFACE

This research effort was sponsored by the Air Force Office of Scientific Research and the Armstrong Laboratory, Crew Systems Directorate, Human Engineering Division, Design Technology Branch (AL/CFHD), Wright-Patterson Air Force Base, Ohio. The work was performed under the Research and Development Laboratory Contract Number F49670-93-C-0076. Support for this work was also provided by Ohio University, Athens, Ohio.

This report was prepared by ***SYTRONICS, Inc.,*** Dayton, Ohio for the Armstrong Laboratory, Design Technology Branch (AL/CFHD) under the Scientific Visualization of Anthropometry for Research and Design (SVARD) Contract Number F41624-93-C-6001.

The authors gratefully acknowledge the assistance of all the members of the Human Engineering Division of Armstrong Laboratory for their support and resources.

TABLE OF CONTENTS

LIST OF FIGURES

LIST OF FIGURES (Cont'd)

LIST OF SYMBOLS, ABBREVIATIONS, AND ACRONYMS

CAD	Computer Aided Design
CARD	Computerized Anthropometric Research and Design
CCD	Charge Coupled Device
CNC	Computer Numerically Controlled
4D VGX	Silicon Graphics Model Number
IGES	International Graphics Exchange Specification
max	Maximum
MHz	Mega Hertz
mm	Millimeter
min	Minimum
PC	Personal Computer
RGB/PS-D	Color Camera with Motion Platform Version D
3-D	Three-Dimensional
$\ominus$	Erosion
f	Signal that is a function of x
g	Structuring element signal that is a function of x
x	The x axis (time)
y	The y axis (Hz)
g_x	Origin of the signal g is positioned at x
$\oplus$	Dilation
$(g\hat{})_x$	Reflection of the structuring element signal g as a function along x
$\bigcirc$	Opening
r	Radius

THIS PAGE INTENTIONALLY LEFT BLANK

SECTION 1.0 - INTRODUCTION

Many technologies exist for capturing surface data including laser scanning, moire fringe topography, and raster stereophotogrammetry. Applications which have benefitted from the use of these surface scanning technologies include facial plastic surgery (Vannier et al., 1991; Young et al., 1994) and the design of equipment which must meet, very closely, the contours of the human body. Such equipment includes prosthetics (Houston et al., 1992), orthotics (Whitestone et al., publication in progress), helmets (Robinette and Whitestone, 1994), masks, clothing, and gloves.

The Computerized Anthropometric Research and Design (CARD) Laboratory of the Human Engineering Division at Wright-Patterson Air Force Base, Ohio has employed a Cyberware Color 3-D Digitizer, a laser scanning system well suited for capturing human head scans, to acquire surface data of the head and face. Figure 1 illustrates a head scan image using the Cyberware scanning system. Currently, the CARD Laboratory maintains a data base of over 1000 surface scan images of the human head which includes both military and civilian personnel. These images, obtained with the Cyberware system, are used extensively for designing head-related equipment.

If a designer of oxygen masks requires scans of the oral-nasal area, the data base can be searched to determine which scans contain high quality surface data from this area. The relevant surface information is extracted from the chosen scans, formatted appropriately for the designated computer-aided design (CAD) environment, and ported to the CAD system. If, however, the data base does not include enough scans with high quality data from the oral-nasal area for the population the designer wishes to sample, a method to correct the scans with poor quality data is required. The removal of one typical degradation, impulse noise or "spikes," is the subject of this paper.

The use of the data base is not restricted to the generation of CAD models; it also can be used to manufacture physical representations of the data. For instance, the data

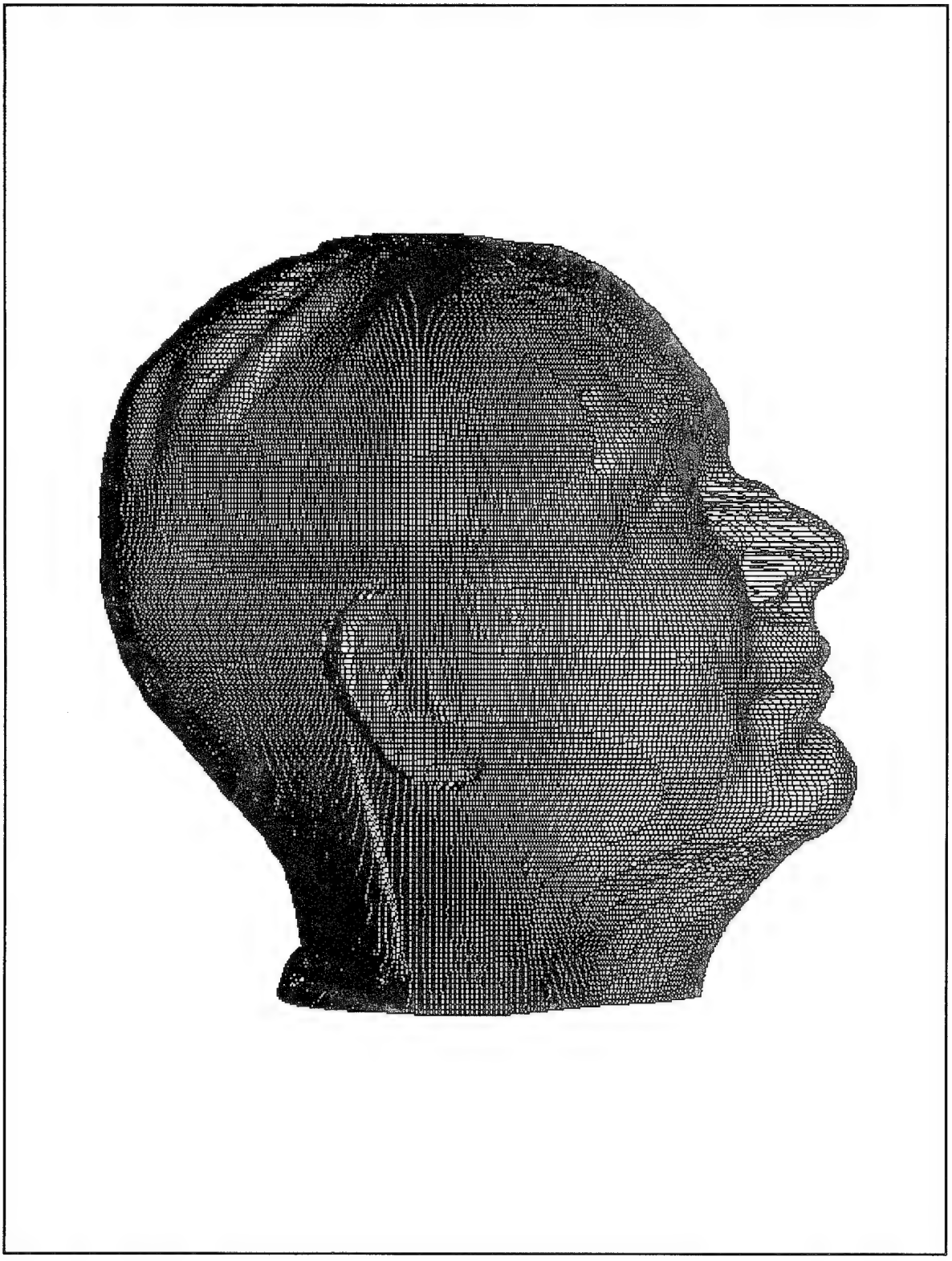

FIGURE 1. Acquired Head Scan Data Points

can be formatted for computer numerically controlled (CNC) milling for rapid prototyping to produce physical models which are used to "mock-up" designs. Once again, a method to correct corrupted data is needed to maintain the integrity of the prototype.

Finally, surface scanning technology can be used in conjunction with visualization and analysis software to provide a unique tool for evaluating virtual prototype systems. Separate scans of the subject and the equipment, when aligned, provide an insightful and quantitative visualization tool for examining the subject/equipment interface and evaluating the "fit" of the equipment (Whitestone, 1993). Shown in Figure 2 are two scans of the same subject which are registered using the common facial surface areas. Landmarks or fiducials common to both scans are registered using a least squares fit, and the process of identifying these landmarks is particularly sensitive to erroneous data acquisition.

Anomalies associated with acquisition can include spikes, voids, and rough surfaces. As these anomalies are embedded in the shape information contained in the image, it is important to try to correct for the spurious data without degrading the rest of the scan. Indiscriminate smoothing of the head scan to remove these anomalies can cause significant changes in the shape of high frequency structures including the nose, ear, jawline, and eye sockets. Because these are the same areas where equipment fit is most critical, extremely sophisticated methods for smoothing the data are required. Furthermore, as these anomalies are widespread throughout the data base, the methods for smoothing the data must be robust in order to apply them globally whenever possible.

This is the second in a series of reports documenting methods used to correct for the spurious results associated with surface scan data (Fang and Nurre, report in preparation). The focus of this report is the method of eliminating spikes or impulse noise in the data while still maintaining the shape information. To eliminate these

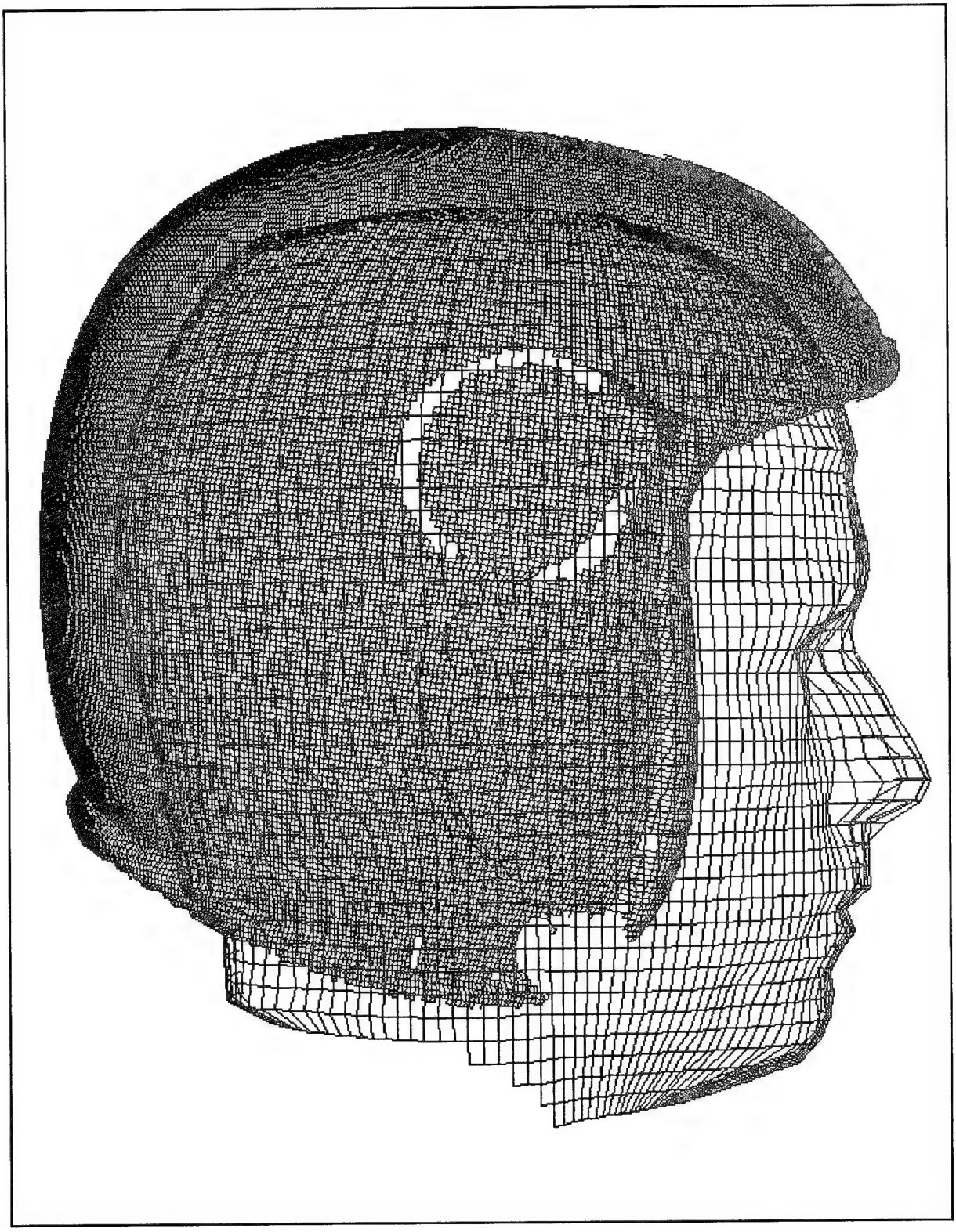

FIGURE 2. Two Separately Scanned Data Sets After Registration

spikes, a morphological filtering technique is presented which takes advantage of the topography of the head. The technique is general enough to be applied to facial plastic surgery and the design of equipment which must meet, very closely, the contours of the human body such as prosthetics, orthotics, helmets, masks, clothing, and gloves. It can also be applied to other scanning methods as well.

The remainder of this report is organized as follows. Section II discusses the data acquisition process and the sources of the errors to be addressed in this report. Section III will present an overview of published research currently being conducted in this field. Section IV presents an approach that is shown to be effective at correcting impulse noise in the data. This section is divided into a mathematical description of morphology, the pertinent head topography, the influence of head topography on morphological filter design, and implementation issues for morphology in a cylindrical coordinate system. Section V will show sample results of correcting the head scan data; Section VI will present a conclusion; and Section VII will discuss topics for future research.

SECTION 2.0 - DATA ACQUISITION

The Cyberware Color 3-D Digitizer Model 4020 RGB/PS-D employed by the CARD Laboratory is capable of acquiring over 130,000 three dimensional points on the surface of the head and face in about 17 seconds. This scanning system, which operates on the principal of triangulation, projects a vertical plane of Helium-Neon laser light on the subject, the profile of which is reflected onto two separate mirrors as the system rotates about the subject's head. The mirrors are aligned such that the separate contours reflected from each are merged into one contour and then projected onto a charge coupled device (CCD) to generate a video image. This redundancy allows surfaces to be captured which might be obscured in one mirror by structures, such as the nose, as the scanner rotates around the subject's head. The contour imaged by the CCD is digitized in a raster fashion and 256 points are identified at regular intervals along the contour. This is repeated for 512 contours spaced at 0.012 radians (≈0.7 degrees) along the full 360 degrees. The resulting contour data is stored as an array, 512 x 256, of 16-bit integer radius values from the center of rotation (approximately, the center of the head). The resolution is 1.563mm in the vertical (longitudinal) direction while the resolution in the horizontal (latitudinal) direction (0.7 degrees of arc) depends on the distance of the surface from the center of rotation. Typically, for the surface of the head, this resolution is about 1.5mm.

As the Cyberware Color 3-D Digitizer does not work well on rough dark surfaces, such as hair, the subject is fitted with a bald cap to provide a smooth, light colored surface that compresses the hair. The subject's head is then centered with respect to the scanning system. A head steadying device is positioned on the top of the head to prevent subject movement when the scan is conducted. The scan data is collected using a Gateway 2000 4DX-33V, a 486/33 MHz PC, which has been equipped with Silicon Graphics Iris Vision boards. This is, in effect, a workstation which is used to quickly visualize the data. For data analysis, however, the data is ported to a Silicon

Graphics 4D 220 VGX workstation. An in-house developed software package called INTEGRATE is used to visualize, analyze, and manipulate the image data.

The spikes or impulse noise encountered during scanning are primarily due to two sources. The first source is external stray light. The light frequency produced by the Helium-Neon laser light source is present in sunlight and incandescent light. As a result, illumination from sunlight or incandescent lights can cause a false detection of the laser beam, resulting in large impulses in the data. The problem of the external light sources is particularly prevalent for a large group of head scans obtained during a survey performed at Eglin Air Force Base. While acquiring these scan data, a door in the scanner room was repeatedly opened and closed. At the time of the measurements, it was not known that the light coming in from the door would introduce a continuous grouping of spikes in the data, such as those shown in Figure 3. Removing these spikes with post processing has a large economic advantage over reconducting the scanning survey.

A second source of impulse noise is large particles floating in the air. The laser beam from the scanner can occasionally illuminate a dust particle in its path. This dust particle is then chosen as the location of the surface at that point, resulting in a spike. The direction of the spike is always external to the surface of the head (i.e. pointing outward). An example of this type of spike is shown in Figure 4.

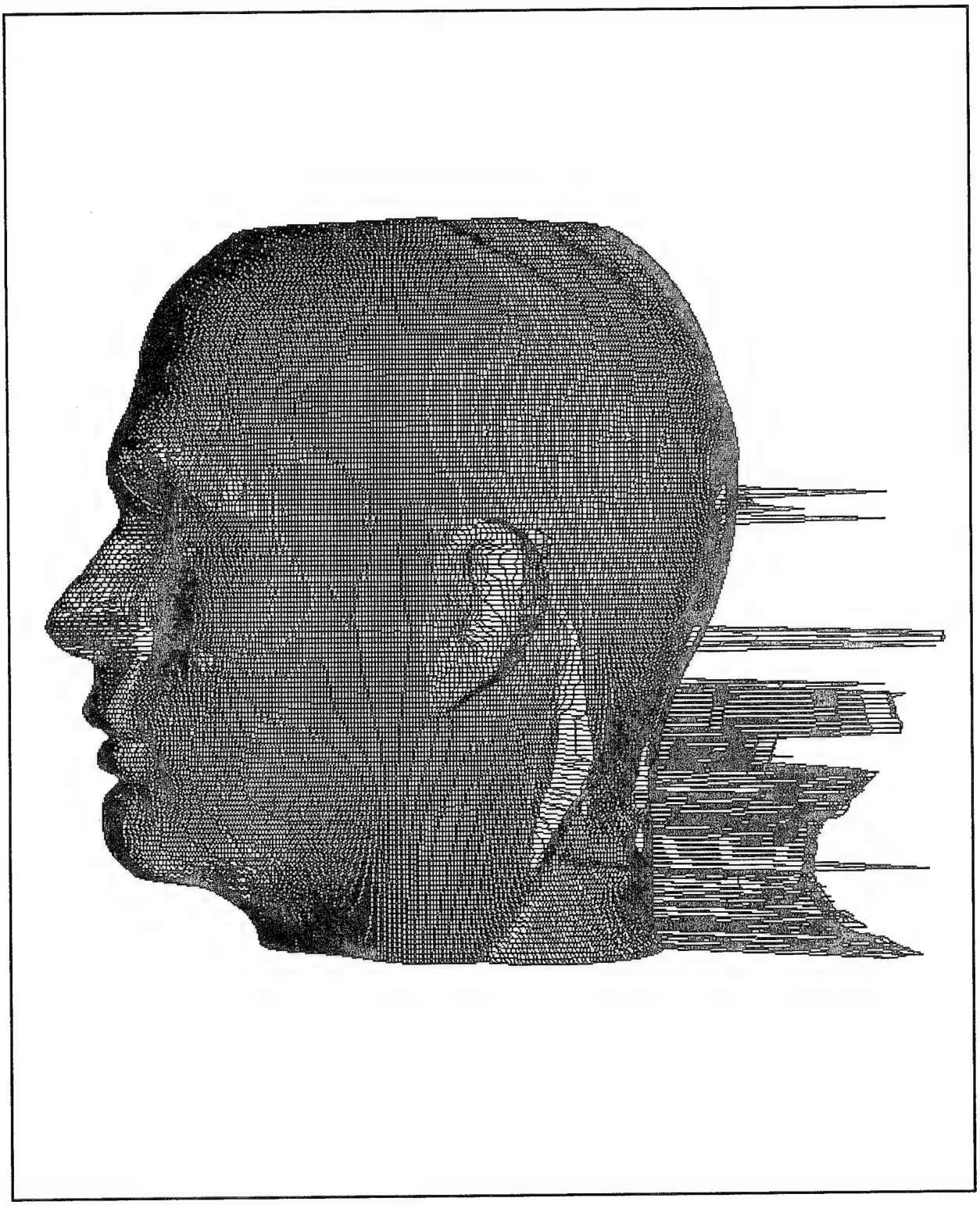

FIGURE 3. A Sample from the Eglin Head Scan Survey. Notice the Continuous Groupings of Spikes Due to an External Light Source.

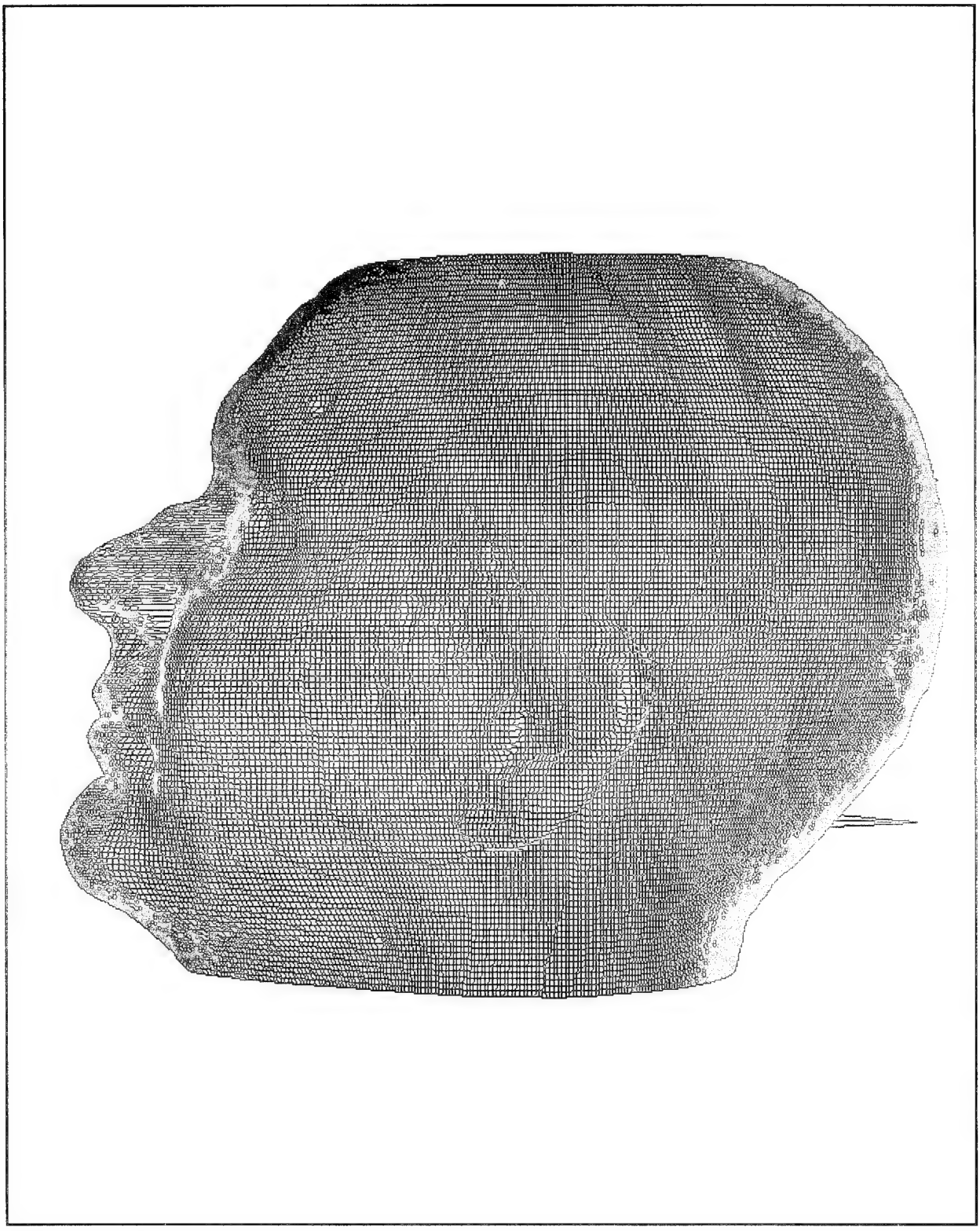

FIGURE 4. Impulse Noise Due to Illumination of a Particle Not on the Head.

SECTION 3.0 - RELATED WORK

Post processing of head range data is beginning to attract the attention of researchers. The topic is usually included in the field of image processing and many techniques are available. However, one unique feature of the head scan data is its cylindrical coordinate system. This requires special software design techniques. Two commonly used techniques for eliminating spikes from two dimensional data are median filtering and morphology (Pratt, 1991). The morphological approach will be used in this report and a comparison will be made to median filters.

Research specifically directed on processing human head scan data has been limited. Gordon (1991) attempted to identify and label head scans through their facial characteristics. To achieve this goal, she has investigated different filtering techniques. Terzopoulos and Waters (1993) have attempted to use head range data to create a synthetic face model. The range data is processed to create deformable contours. Nurre (1993) has previously experimented with regularization techniques to remove noise from head range data. Pavlakos et al. (1989) discuss a method for converting head scans into the IGES format. The methods discussed in this report would represent a pre-processing step to any of the research mentioned above.

SECTION 4.0 - THEORY AND DEVELOPMENT

Section 4.1 - Introduction to Morphology

The study of form and structure in biology is commonly referred to as morphology. In the area of image processing, mathematical morphology refers to a branch of nonlinear filters developed by Matheron which also uses form and structure (Matheron, 1975). Specifically, mathematical morphology is the probing of an image shape with a specified structuring element. The geometry of the structuring element implies certain geometric characteristics about the image being analyzed.

Choosing among the large number of structuring elements, to find an appropriate one for a given application, is a critical part of morphology. The number and types of operations performed by any structuring element are limited, however, and quite specific. Two operations, erosion and dilation, will be briefly introduced below. These operations which have been implemented in INTEGRATE, the head scan analysis software package, can be used to perform a filtering operation known as opening, also described below. Further information on morphological techniques and the theory of mathematical morphology can be found in references by Dougherty (1992), Dougherty and Giardina (1987), and Serra (1988).

As stated earlier, morphology concerns itself with the probing of a signal with a geometric structuring element. An erosion fits the element to the signal. To find the erosion of a signal by a structuring element, the element is placed below the signal and forced up to the highest elevation which will touch but not cross the signal. The origin of the element becomes the new signal value. The process is repeated throughout the length of the original signal. The erosion of the signal is defined mathematically as:

$$(f \ominus g)(x) = \max\{y : g_x + y << f\} \qquad (1)$$

For the definition, x and y represent a standard axis system with x being the independent variable and f, g being functions of x. The structuring element is signal g, and g_x refers to the origin of the signal being positioned at x.

An erosion of two one-dimensional signals is shown in Figure 5. The structuring element is the right triangle, represented by signal g. Notice the origin of g falls at the 90 degree angle as shown in the left of Figure 5. This will become the new location of the eroded signal. The f signal to be eroded is represented by the solid line shown in the right hand of the figure while f $\ominus$ g is represented by a dashed line.

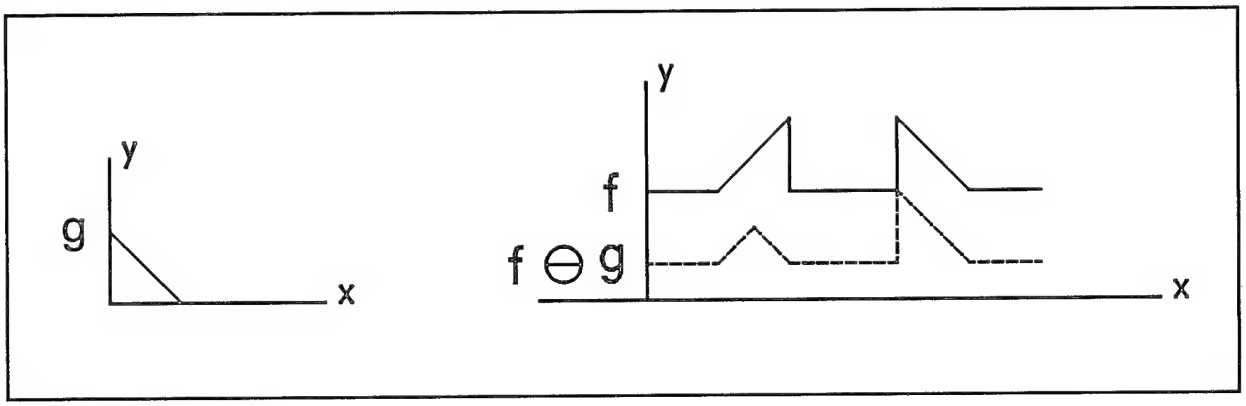

FIGURE 5. The Signal g is the Structuring Element for the Erosion of Signal f.

Dilation is the dual operation to erosion. When dilating a signal with a structuring element, the signal becomes a path for the origin of the element. As the element translates its path, a new signal is created which is the minimum signal needed to bound the structuring element. Another method for finding the dilation is reflecting the structuring element across the x = y axis and finding the minimum signal above the original signal in which the reflection will fit. From this method, a mathematical description of dilation can be defined as:

$$(f \oplus g)(x) = \min\{y:(g\hat{})_x + y >> f\} \qquad (2)$$

where (g^) is the reflection of the structuring element.

A dilation of two one-dimensional signals is shown in Figure 6. The structuring element is once again a right triangle as presented previously. The f signal is represented by the solid line shown in the right hand figure while f ⊕ g is represented by a dashed line.

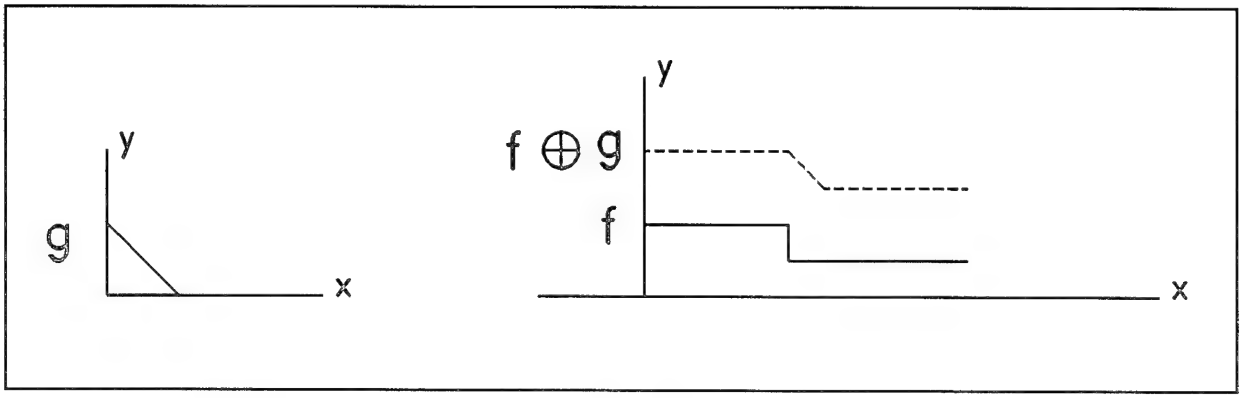

FIGURE 6. The Signal g is the Structuring Element for the Dilation of Signal f.

An opening filter operation is defined as an erosion operation followed by a dilation. An opening with the proper structuring element is especially effective at removing spikes appearing above the local signal level (Dougherty, 1992). The opening of signals is defined mathematically as:

$$(f \bigcirc g)(x) = (f \ominus g) \oplus g \qquad (3)$$

In Figure 7, the signal has two spikes above the local signal level, which can be removed with the structuring element shown as signal g. In essence, the spikes are removed due to the fact that the structuring element does not fit within the spikes' area. It is important to point out in this simple example that the signal, except for the spikes, was unchanged. This is the type of operation desired to remove impulse noise from head scan data without corrupting the data. Opening a different signal, with the

same structuring element, may result in unwanted corruption of the data, as shown in Figure 8. Hence, the structuring element must be appropriately chosen to discriminate between spikes and good data points.

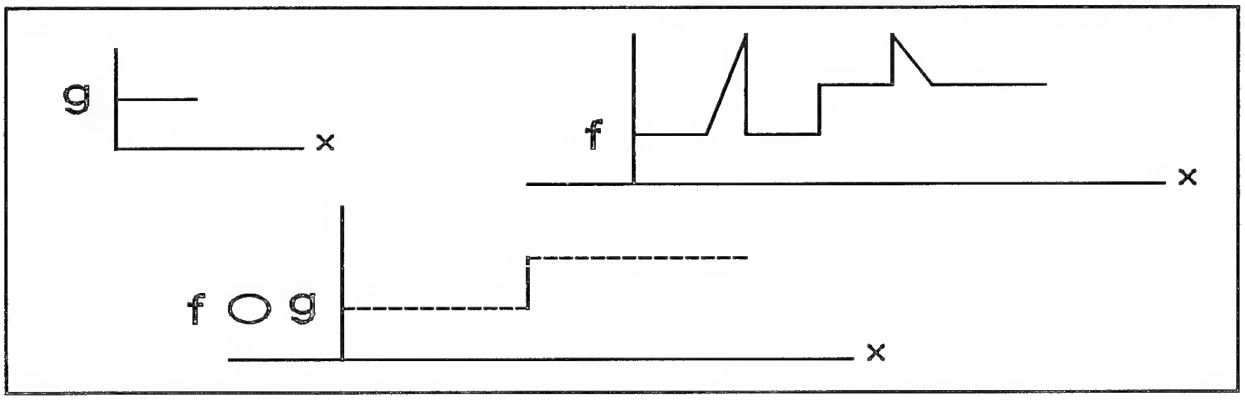

FIGURE 7. The Opening of Signal f and g, to Remove Spikes from f.

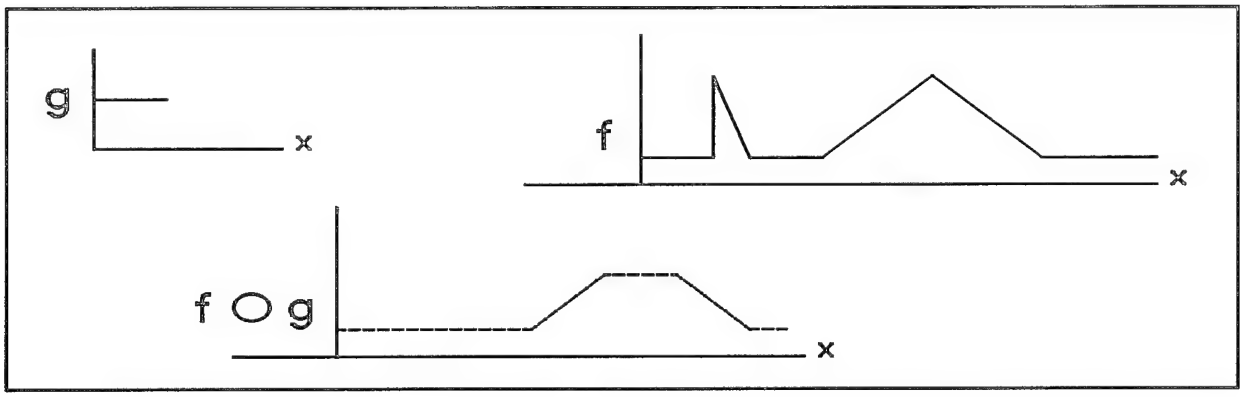

FIGURE 8. Using a Morphological Opening to Remove Spikes Can Have Undesirable Consequences as Shown.

Section 4.2 - Human Head Topography

As will be demonstrated, understanding the topology of the human head will help define the problem of identifying and thus removing impulse noise in head scan data. The head will be characterized beginning externally with the surface captured by the

scanning process and continuing to the underlying structure of the rigid bone. This characterization will allow structuring elements to be chosen that will result in spike removal when applied to the scan data.

The scanner captures the surface of the skin. Skin is the largest organ in the body and can be divided into two major tissue layers, the epidermis and dermis. The epidermis is the thinner, outer layer and can be subdivided into four layers. The outermost layer of the epidermis, the stratum corneum, is a thin layer of dead cells which is exposed to the environment. The dermis, which is thicker and composed solely of living tissue, gives skin most of its biomechanical properties. Because of the dermis, skin can be modelled with a biphasic stress-strain curve (Odland, 1983) as a highly elastic tissue under low stress.

The composition of the tissue underlying the skin is dependent on its location on the head. The soft tissues of the human head can be divided into a scalp or cranial portion and the face. In the scalp region, which starts at the upper portion of the skull and continues posteriorly over the head to the beginning of the neck, the skin is covered by hair and adheres closely to the skull (McClintic, 1975). The skin in this region thins from its average thickness of approximately 2mm to approximately 1.5mm (Larrabee, 1986). Also, there are few muscles and little fat in the subcutaneous tissue of the scalp to separate the skin from the underlying skull. The skin of the face, on the other hand, is separated from the underlying bone by more than 200 voluntary muscles, and the skin thickness is approximately 2mm.

The scalp region is compressed by a bald cap. The bald cap itself is elastic and 0.5mm thick. Combining the 1.5mm thick skin of the scalp, the compressed hair, and the bald cap, it can be seen that the surface captured by the head scanning process in the scalp region can be considered to be an elastic layer at least 2mm thick overlying the skull.

As stated earlier, the face region is covered by approximately 2mm of skin and varying amounts of subcutaneous fat and muscles all of which are loosely connected to the underlying bones of the face. Therefore, the surface captured by the head scanning process can be considered an elastic layer at least 2mm thick overlying and connected to a more rigid underlying structure.

The derivation of the above surface model will be used to characterize the possible shapes of structures, on the scanned subject's head, that should not be identified as spikes. As explained in the Introduction, impulse noise always occurs externally from the head. Therefore, the discussion will be limited to structures of the scanned subject's head that project externally. Most protruding structures on the head are the result of infection or some other space occupying mass under the skin. Since the skin model will cover these structures, they must have a base of at least 4mm as shown in Figure 9 and as explained below.

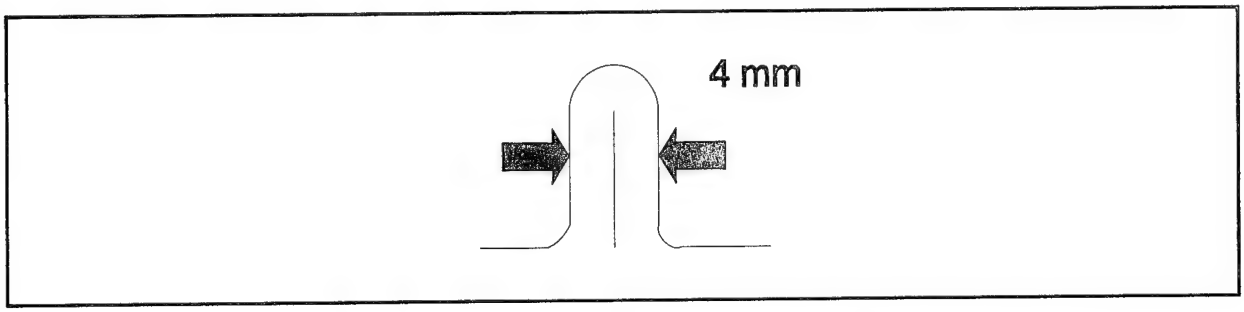

FIGURE 9. Minimal Size of a Protruding Structure on the Head Derived from a Structure Beneath the Skin Model

The structure shown in Figure 9, consisting of a highly elastic material, could not be supported against gravity. The central core of the protruding structure must have enough width and strength to support the skin against gravity. On the other hand, lesions which occur within the skin, such as warts or blisters, could violate the above assumptions and produce a protruding lesion with a diameter smaller than 4mm. These structures can be noted by the scanner operator. None of the head scans used

in this paper contained such lesions. Therefore, spikes in the data with a diameter less than 4mm are likely to represent impulse noise. This fact can be used in designing an appropriate structuring element.

Section 4.3 - Morphological Filter

Consequently, the problem of removing impulse noise from human head scan data has been reduced to removing outward pointing spikes with a diameter less than 4mm. Therefore, opening with a structuring element whose diameter is no greater than 4mm in size should result in the desired solution. In essence, the failure of an element to fit into a spike during erosion will result in the spike's elimination. Structuring elements larger than 4mm in diameter, on the other hand, may fail to fit into actual head features and would result in corruption of the data.

The opening operation is to be performed on cylindrical range data. The axis of erosion is the radial axis. In other words, the structuring element will be "pushed up" in the radial direction. The base of a spike is not necessarily perpendicular to the radial axis. Therefore a structuring element with an omni-directional behavior is required. An element which fails to fit a specified diameter in any direction would be a sphere. Figure 10 shows the structuring element, a sphere, where its origin is specified by radius, r.

The desired structuring element should be such that the dilation results in an accurate interpolation with neighboring points. Most points on the surface of the head will fall into smooth convex regions. Use of a spherical structure will result in a convex interpolation of the impulse noise data. Furthermore, the spherical structure itself is smooth. The curvature of a 4mm sphere, however, may be higher than the curvature of regions on the face. Poor interpolation values may result when the corrected impulse data has a curvature different from that of the sphere in these areas.

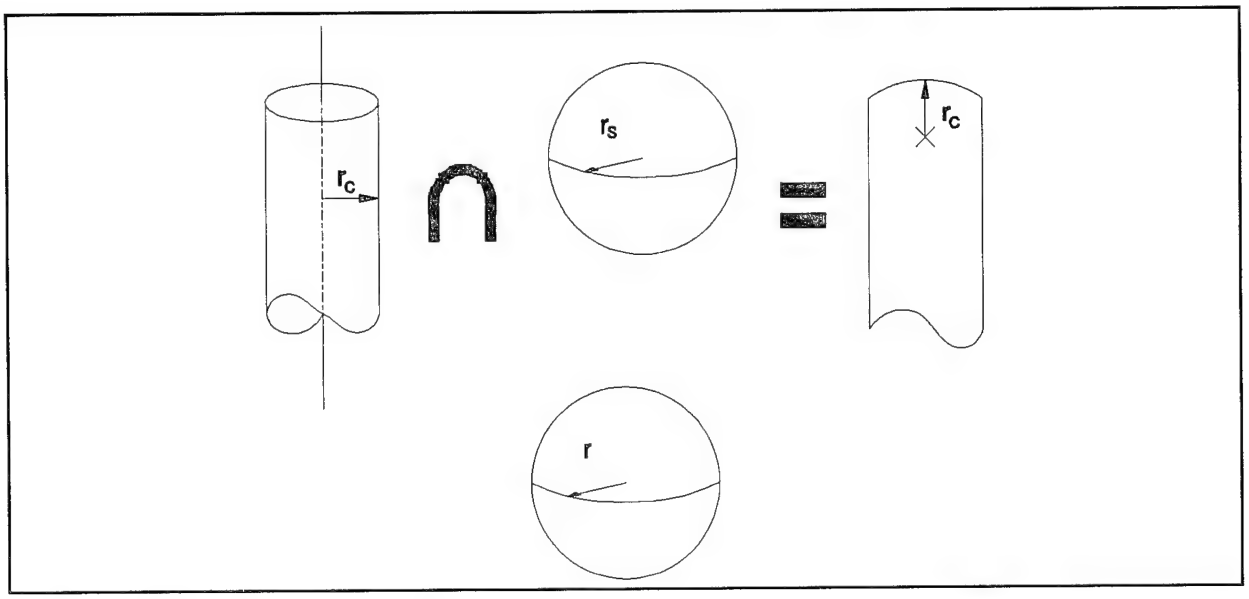

FIGURE 10. A Spherical Structuring Element Satisfies the Requirements for Spike Removal on the Head Scans

Section 4.4 - Morphological Algorithms in Cylindrical Coordinates

Because of the cylindrical coordinate system, the number of points influenced by the structuring element changed depending on their distance from the zero radius axis. Points far from zero are more scattered, when sampling in the radial direction, than closer points. During erosion, the initial position of the origin of the structuring element must be placed at a distance from the zero radius axis equal to the smallest radial value of the effected longitudinal scan, minus the radius of the sphere. The element was pushed up from this point with fewer points required for checking as it moved. Dilation was similarly executed. As the sampling resolution in the vertical direction is 1.563mm, a structuring element with a base size smaller than this resolution may be constrained by only a single point at larger distances. Therefore, the 1.563mm value can be considered the minimum value for r.

SECTION 5.0 - RESULTS/APPLICATION

Section 5.1 - Determining Optimal Filter Size

As stated earlier, the problem of the external light sources is particularly prevalent for a large group of head scans obtained during a survey performed at Eglin Air Force Base. Removing these spikes with post processing has a large economic advantage over reconducting the scanning survey. Another source of sporadic spikes is introduced by large floating particles in the air.

In this experiment, five head scans that were relatively free of random spike noise were chosen. An experienced operator reviewed the head scans and set to zero any remaining spikes. (INTEGRATE is designed to ignore any data points set to zero.) These five head scans will be referred to as the ideal data set.

Seventeen additional head scans were chosen with varying degrees of impulse noise corruption. Once again, an experienced operator reviewed the head scans. All spikes for the seventeen scans were identified, and the difference between the data point's corrupted location and the average position of its neighbors was recorded. Figure 3 showed one of the seventeen head scans analyzed. The impulse noise data obtained from this scan is displayed in cylindrical coordinates and shown in Figure 11.

The noise data from each of the seventeen scans was added to each of the ideal scans, one at a time. Figures 12 and 13 show one of the ideal scans before and after one sequence of impulse noise was added. Appendix A displays one of the ideal heads with each of the 17 impulse sequences added separately. An opening with a spherical structuring element of varying size was executed on the newly corrupted data and measurements were recorded.

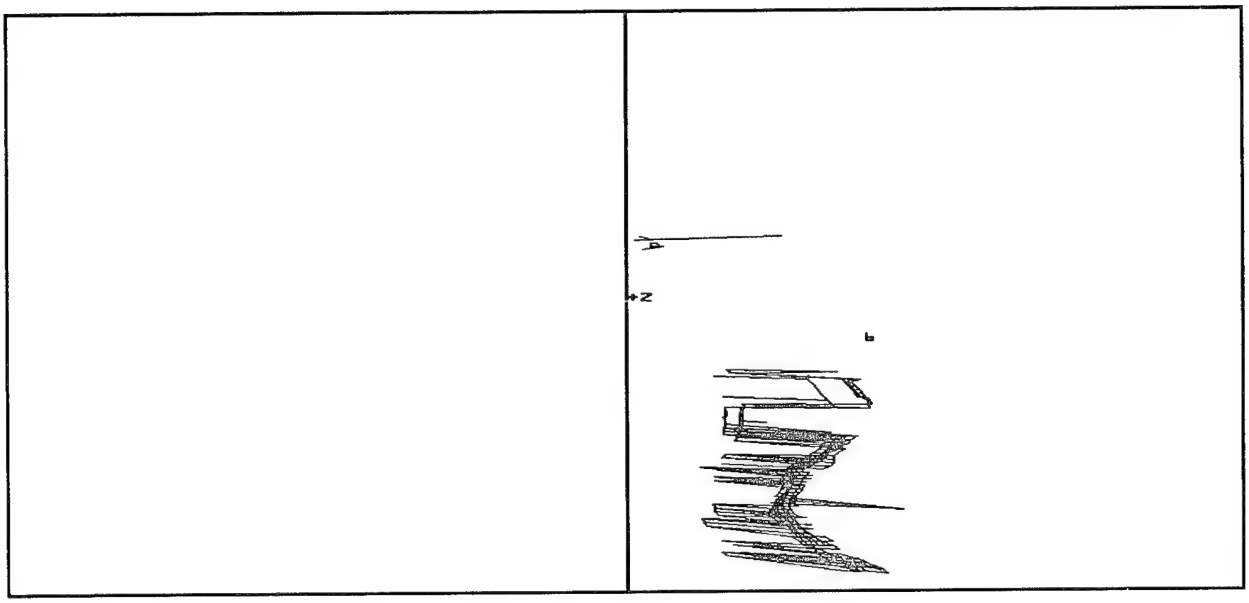

FIGURE 11. Spike Data from the Eglin Head Scan Survey. The Center Line Represents Zero Radius Data.

Two of the measurements recorded indicate the usefulness of the filter for simply identifying spikes. In general, the number of data points obtained from the head is excessive. Identifying and removing spikes, with a small percentage of 'good' points that were incorrectly identified, would be acceptable. In fact, the CARD Laboratory is investigating methods of removing up to 90% of the data points by surface fitting, for better data management.

The three measurements used to judge the performance of the openings were as follows. First, impulse data points which were moved by more than 1mm after the opening were identified as spikes. Second, the opening was judged on its corrupting effect of "good" data points. Ideal data points that were moved by more than 1mm by the opening would also be identified as spikes and therefore are judged to be corrupt. The points will be referred to as "other points moved" in the figures and tables. Third, the opening was judged on its ability to move spike data back to their ideal location. Points that are moved to within 1mm of their original location are considered to have been corrected.

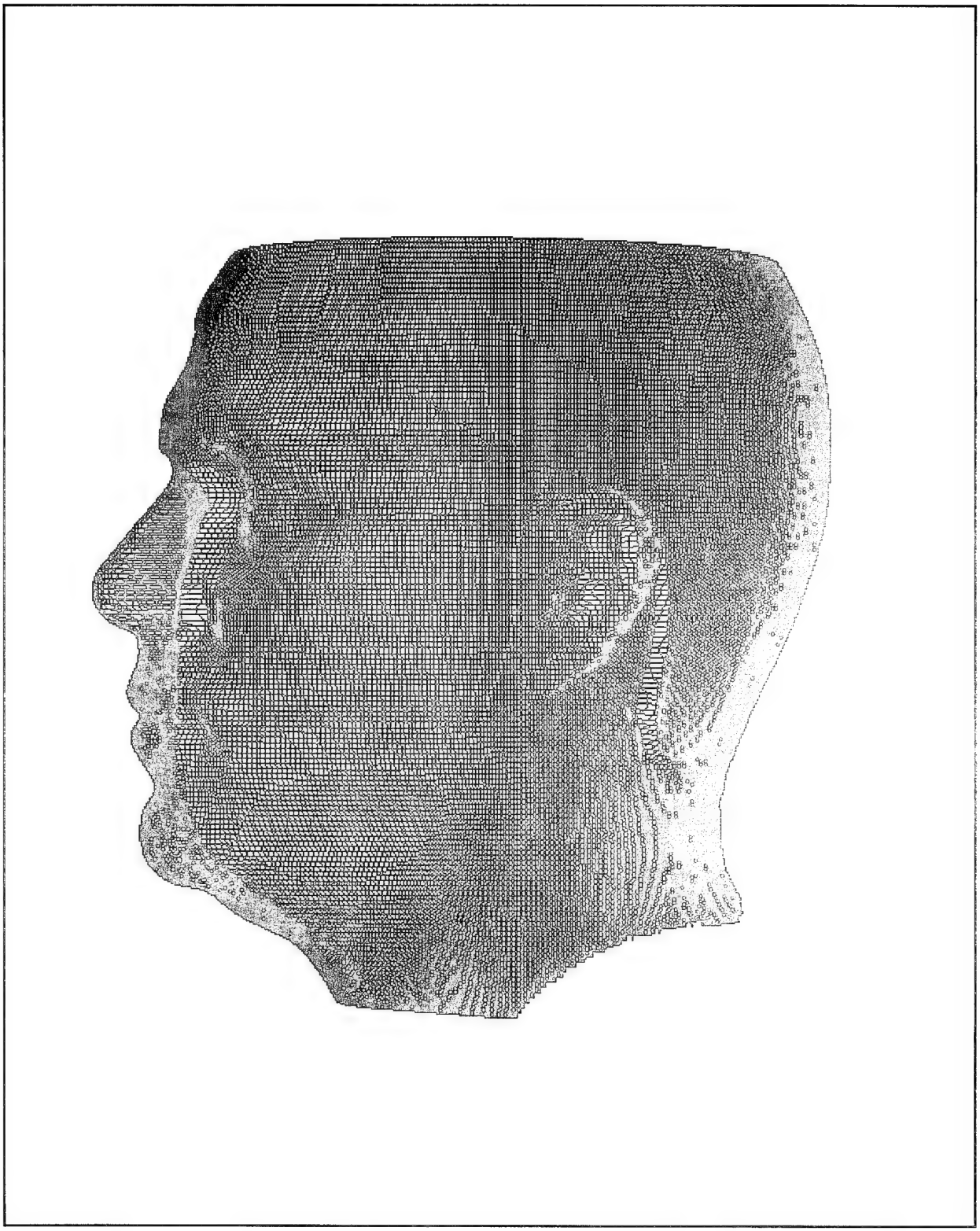

FIGURE 12. An Ideal Head Scan

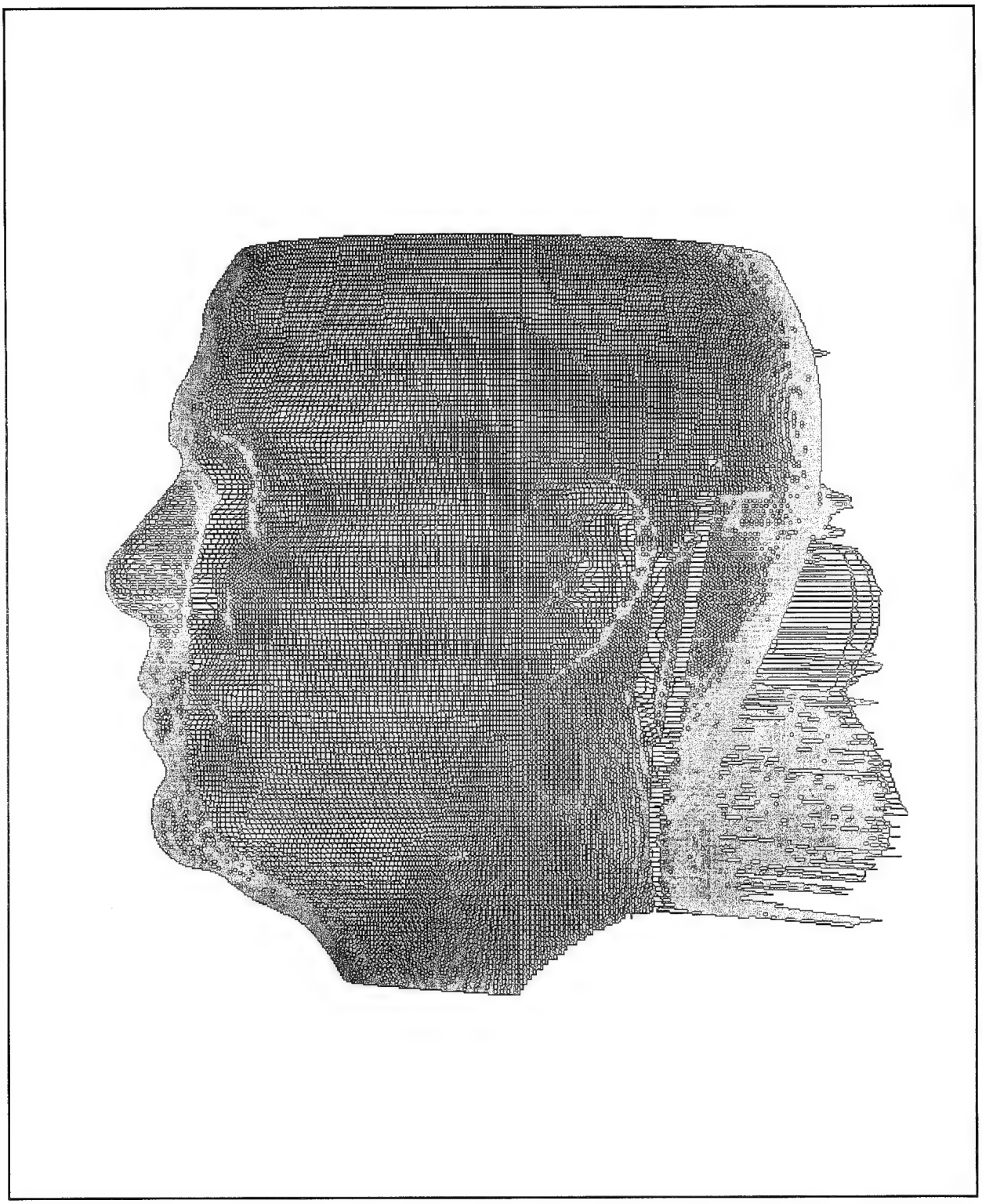

FIGURE 13. The Ideal Head Scan with Added Spike Noise

The Tables in Appendix B show the results of openings of various sizes. The results are given in percentage of nonzero data points affected. The head scans are subdivided by features as shown in Figure 14. When adding the data set of impulse noise to the ideal scans, not all features were affected. For example, a particular set of impulse noise may not contain any spikes in the nose region. When a set of impulse noise was added to an ideal head scan and no spikes were added to a particular region, then this scan was not included in the statistics for that particular part. In the Tables, the average percentage of points affected is given. Contained within the brackets is the standard deviation of the average and the number of impulse data sets these statistics are based on.

The percentage of data identified, corrected and corrupted is plotted in Figure 15, for the entire head. Openings of radial size 3.5mm and greater identified nearly all spikes in all cases. The number of false positive ('good' points that were moved by more than 1.0mm) remained less than 5% for all cases. A size of 3mm appears to be an inflection point on the other moved points plot. Radial sizes between 3.0mm and 3.5mm appear to represent a good trade off between spike identification and loss of mis-identified data. The ability of the opening operation to correct the data steadily improved with increased radial size. At least 80% of the data was corrected for openings larger than 3.5mm.

Figure 16 shows the effects of the opening operation when restricted exclusively to the back of the head. The results for identified and corrected data are similar to the case of the entire head. However, the number of other points moved is negligible for all but one head scan. This particular head scan has a large amount of white noise due to a misalignment of the scanner's mirrors.

Finally, Figure 17 shows the results of the openings on the ears. Assumptions about the head, presented in the previous section, failed to take into account orifices and overlapping structures on the head. Especially problematic are the ears. This is

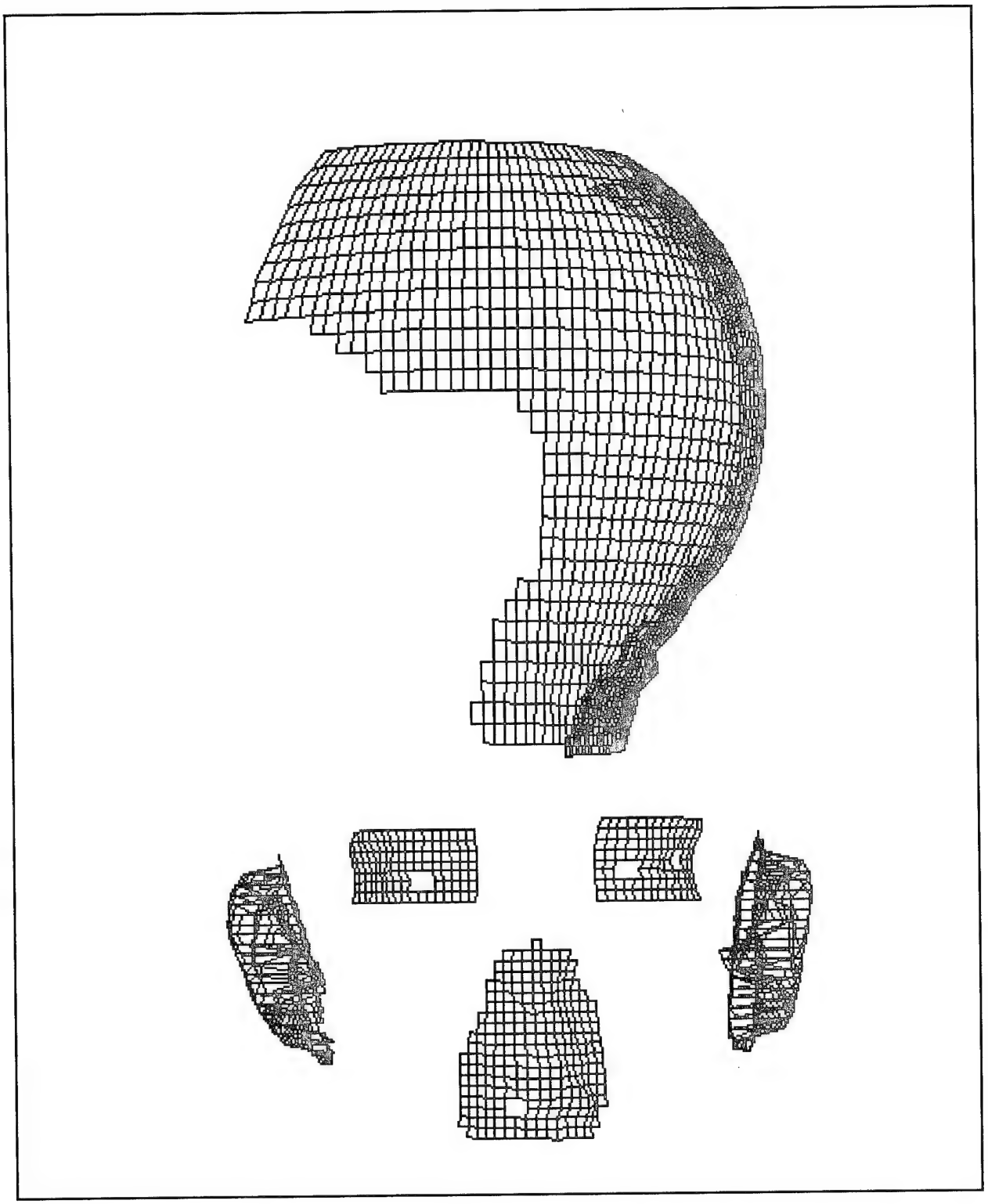

FIGURE 14. Measurements were Taken from the Back of the Head, Eyes, Ears, and Nose

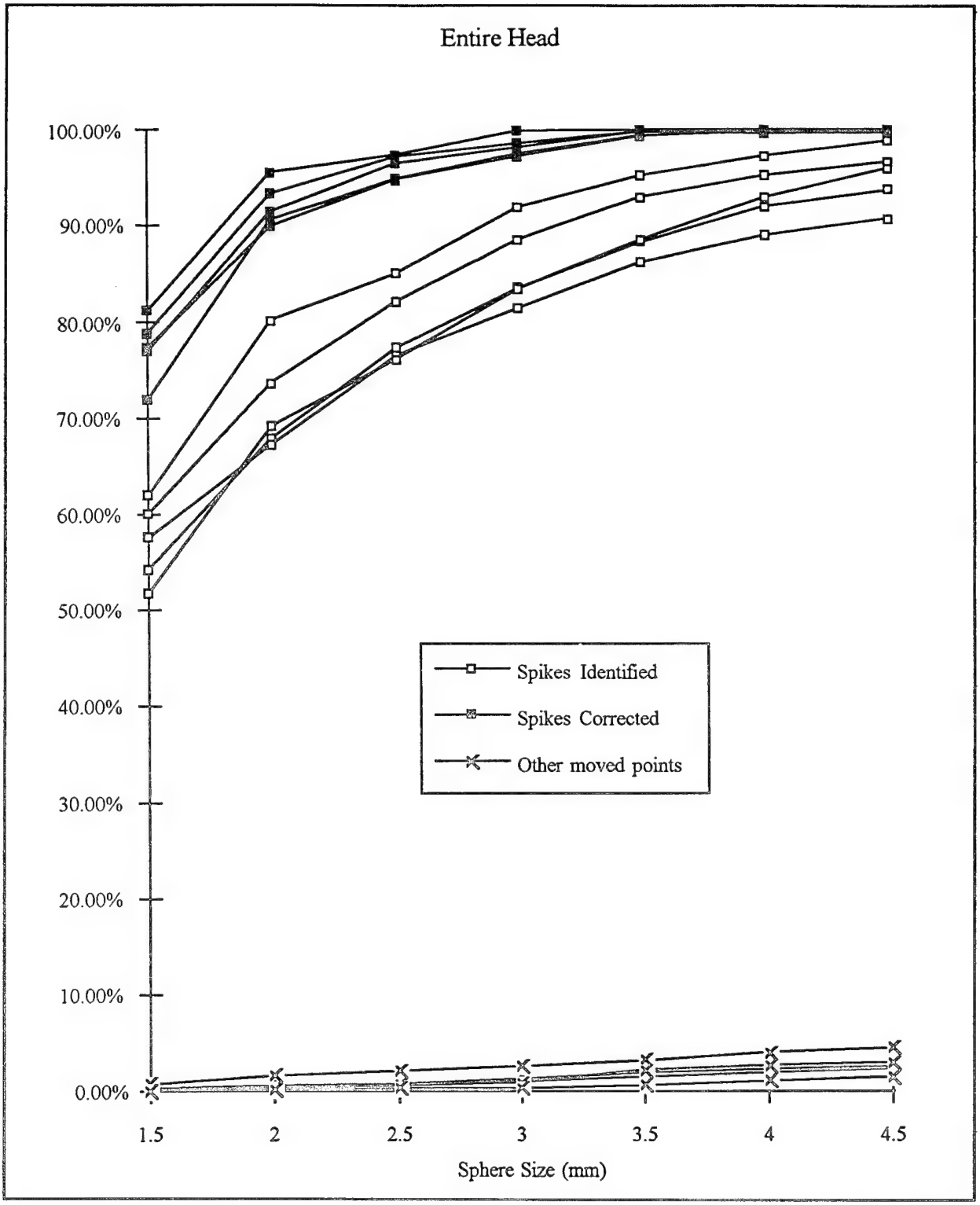

FIGURE 15. Measurements Taken from the Entire Head for an Opening Operation with a Sphere of Varying Size

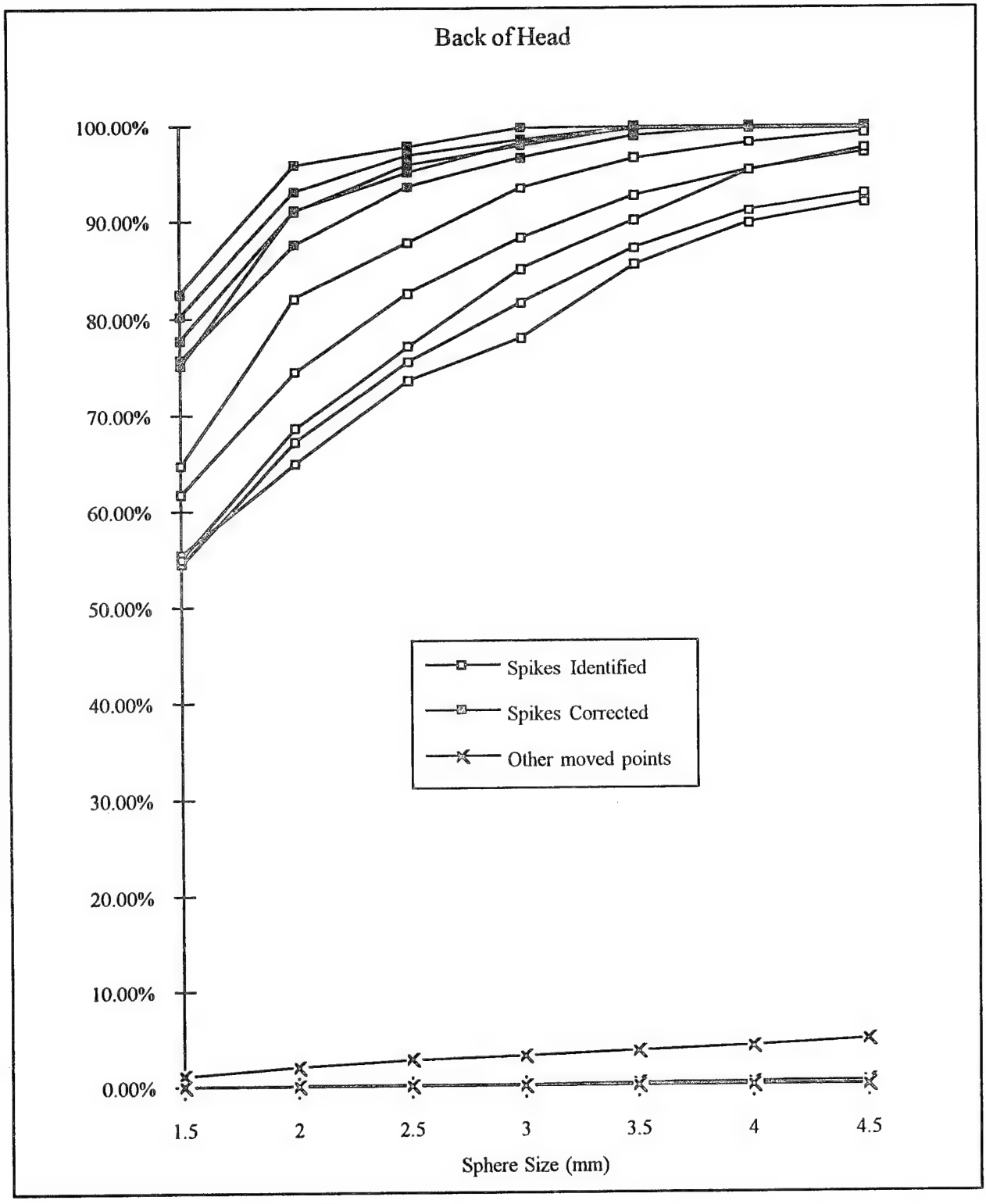

FIGURE 16. Measurements Taken only from the Back of the Head for an Opening Operation with a Sphere of Varying Size

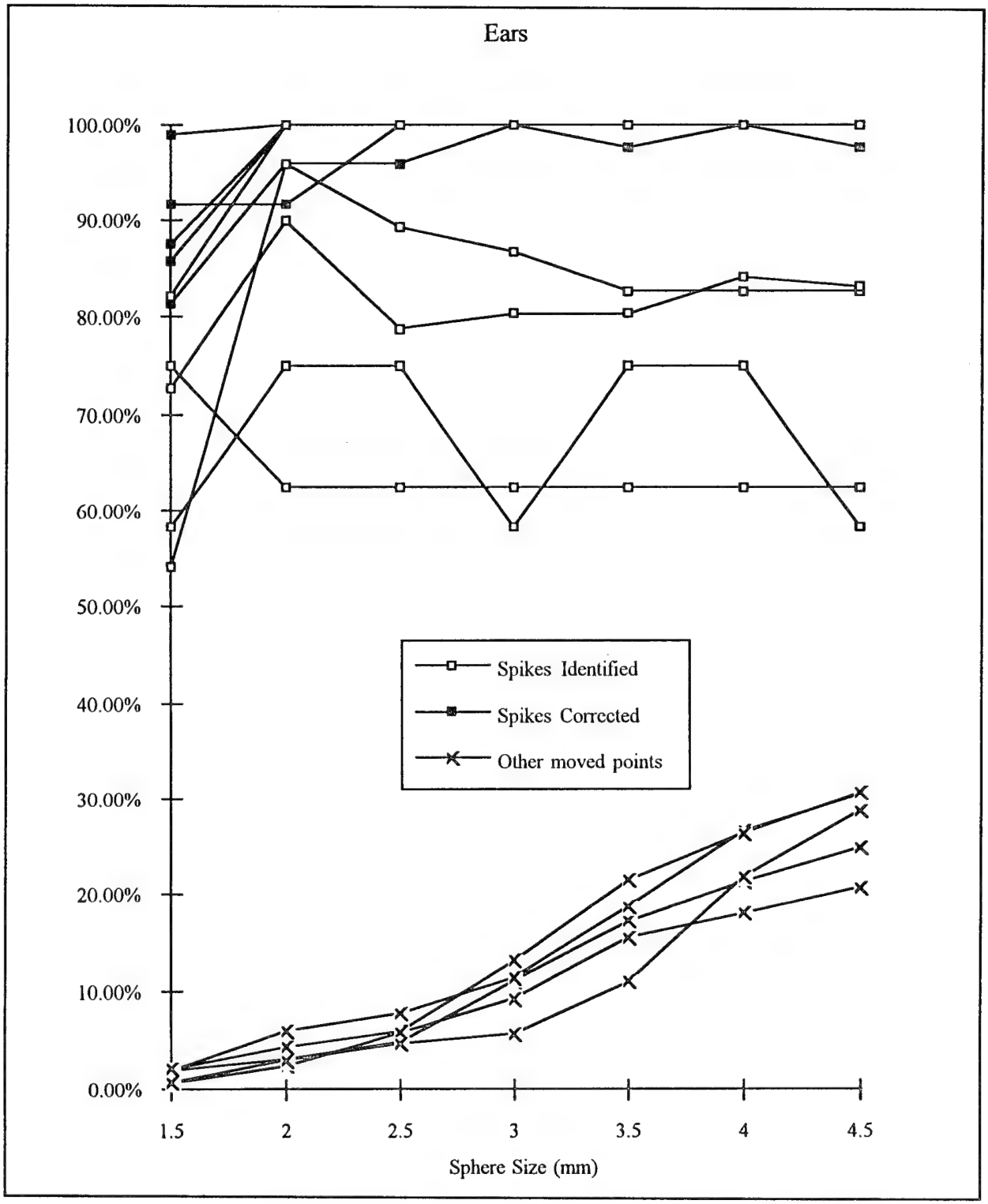

FIGURE 17. Measurements Taken only from the Ears for an Opening Operation with a Sphere of Varying Size

evident in the figure but to a lesser extent than might be expected. The ear canal, for example, appears in the range data as an inward pointing lesion. Inward pointing signals are not greatly affected by an opening. The ear overlap shows up as a step in the range data and its degradation is small. In any case, the range processing software has the option of excluding the ears from the opening operation.

Section 5.2 - Comparison with Median Filter

As a point of comparison, a median filter algorithm was also tested with the head scan data. Median filtering, replacing a center point with the median of its neighbor, is highly regarded as a technique for removing spikes from data. The algorithm requires rectangular data and therefore the cylindrical data had to be 'unwrapped'. The radial angle becomes one axis, and the height becomes the second axis. A circular neighborhood was used to determined the median, for adequate comparison with the morphological operation. It should be noted that morphology and median filtering have been proven to be identical in some limited cases (Maragos and Schafer, 1987). However, in the case of removing impulse noise from human head scan data, the two techniques are not identical. Figure 18 shows a plot of identified, corrected and corrupted data points for six different filter sizes. The percentage of the identifiable spikes is similar to the morphological case. The median filter, however, resulted in a significantly higher percentage of other points being moved. It also failed to correct points at the same rate as the morphological method. An additional drawback to the median filter was its speed which proved to be slower than the opening operation.

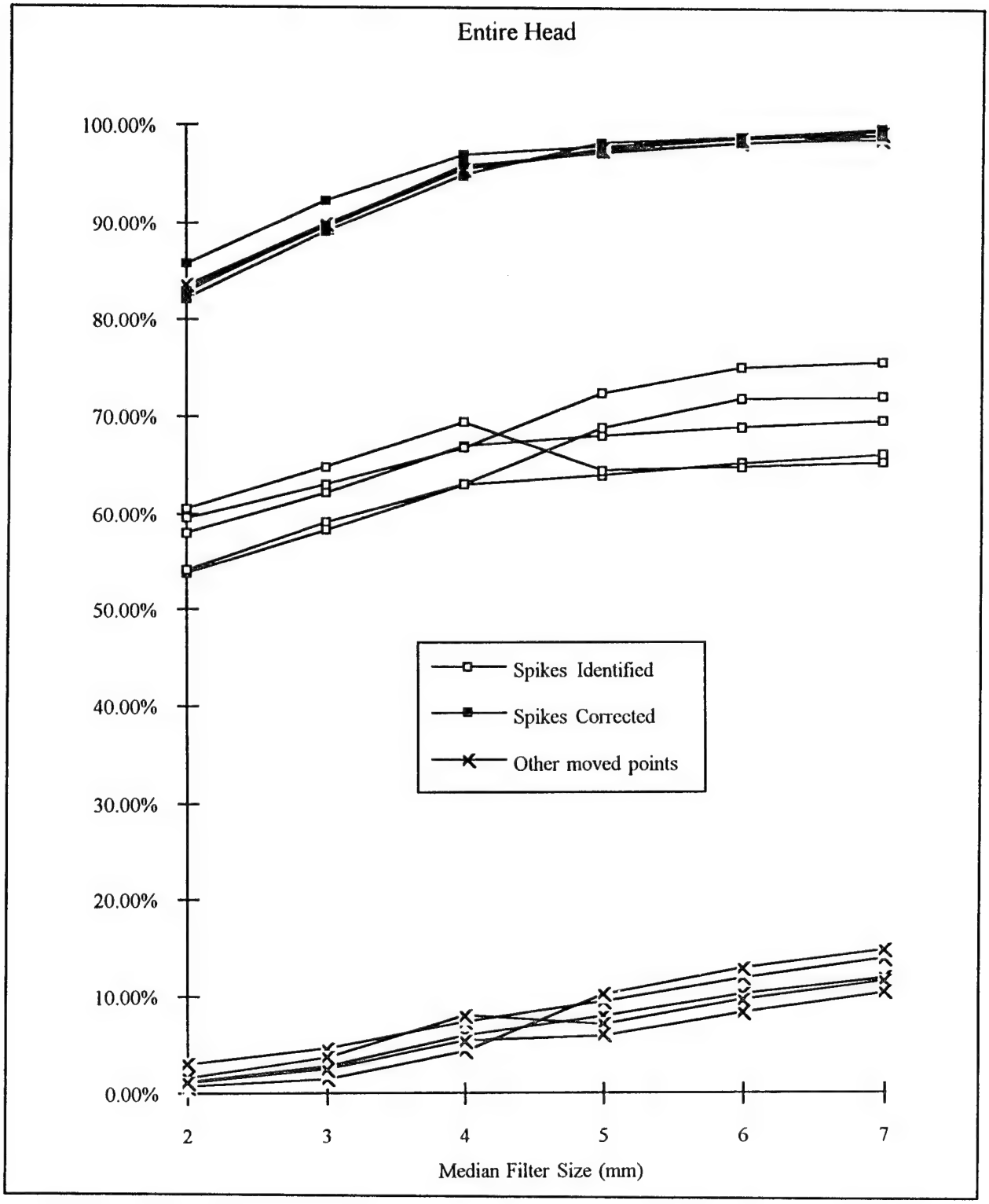

FIGURE 18. Measurements Taken from the Entire Head for a Median Filter Operation with a Sphere of Varying Size

SECTION 6.0 - CONCLUSIONS

Within this research, morphological filtering of head scan data to remove spikes was justified based on physiology. A spherical structuring element of 4.0mm proved to be a slightly conservative radius for the spherical structuring element used. Openings of radial size 3.5mm and greater identified nearly all spikes in all cases while the number of false positives always remained less than 5%. The rate of data corruption appeared to increase at about the 3.5mm size as expected. As a practical matter, therefore, radial sizes between 3.0mm and 3.5mm appear to represent a good trade off between identification and loss of data.

The results for identified and corrected data were less than satisfactory in some localized regions of the head. The ears in particular violated many of the underlying assumptions presented. Therefore, an effective and sound strategy of improving the scan results is to limit the filtering process to exclude the back of the ears.

SECTION 7.0 - FUTURE WORK

The ability of the opening operation to correct the data steadily improved with increased radial size. The larger curvature of the sphere better matched the curvature of the surface of the head in most regions. Design of an element with a small base (to prevent feature loss) but large curvature is needed. One of the primary challenges will be the need for the element to have an omni-directional behavior since the base of a spike is not necessarily perpendicular to the radial axis.

SECTION 8.0 - REFERENCES

1. Doughtery, E.R., (1992). *An Introduction to Morphological Image Processing*. Bellingham, W.A.: SPIE Optical Engineering Press.

2. Doughtery, E.R., and Giardina, C.R., (1987). *Matrix Structured Image Processing*. Englewood Cliffs, N.J.: Prentice-Hall, Inc.

3. Fang, H., and Nurre, J.H. Optimal Estimation of Head Scan Data Using Generalized Cross Validation. Unpublished manuscript.

4. Gordon, G.G., (1991). Face Recognition Based on Depth Maps and Surface Curvature. *SPIE Geometric Methods in Computer Vision*, 1570: 234-247.

5. Gordon, G.G., (1991). Smoothing Range Data for Curvature Estimation. *Active Perception and Robot Vision*, 481-498.

6. Houston, V.L., Burgess, E.M., Lehneis, H.R., Mason, C.P., Garbarini, M.A., LaBlanc, K.P., Boone, D.A., Chan, R.B., Harlan, J.H., and Brncick, M.D., (1992). Automated Fabrication of Mobility Aids (AFMA): Below-Knee CASD/CAM Testing and Evaluation Program Results. *Journal of Rehabilitation Research*, 29(4): 78-124.

7. Larrabee, W., (1986). A Finite Element Model of Skin Deformation I. Biomechanics of Skin and Soft Tissue: A Review. *Laryngoscope*, 96: 399-419.

8. Maragos, P., and Schafer, R.W., (1987). Morphological Filters-Part II: Their Relations to Median, Order-Statistic, and Stack Filters. *IEEE Trans. on Acoustics, Speech and Signal Processing*, 53(8): 1170-1184.

9. Matheron, G., (1975). *Random Sets and Integral Geometry*. New York, N.Y.: John Wiley and Sons, Inc.

10. McClintic, J.R., (1975). *Basic Anatomy and Physiology of the Human Body, 2nd Ed*. New York, N.Y.: John Wiley & Sons, Inc.

11. Nurre, J.H., (February, 1993). Post Processing Cylindrical Surface Data of a Subject's Head. *IS&T SPIE Symposium on Electronic Imaging: Science & Technology*, San Jose, California.

12. Odland, G.F., and Goldsmith, L.A., editor, (1983). *Biochemistry and Physiology of the Skin*. New York: Oxford University Press.

13. Pavlakos, E.G., Greenfield, I., Cutting, C.B., and Wei, C.S., (July, 1989). Conversion of 3D Scan Data to IGES Data Base for Design and Manufacturing. *Proc. ASME Internal. Computers in Eg. Conf.*, Anaheim, California, 99-103.

14. Pratt, W.K., (1991). *Digital Image Processing*. New York, N.Y.: John Wiley & Sons, Inc.

15. Robinette, K.M., and Whitestone, J.J., (May 1994). The Need for Improved Anthropometric Methods for the Development of Helmet Systems. *Aviation, Space, and Environmental Medicine*, A95-A99.

16. Serra, J., editor, (1988). *Image Analysis and Mathematical Morphology, Vol. 2.* New York: Academic Press.

17. Terzopoulos, D., and Waters, K., (1993). Analysis and Synthesis of Facial Image Sequences Using Physical and Anatomical Models. *IEEE Trans. on PAMI*, 15(6): 569-579.

18. Vannier, M.W., Pilgrim, T., Bhatia, G., Brunsden, B., and Commean, P., (1991). Facial Surface Scanner. *IEEE Comp. Graphics Appl.*, 11(6): 72-80.

19. Whitestone, J.J., (1993). Design and Evaluation of Helmet Systems Using 3D Data. Proceedings of the 37th *Annual Meeting of the Human Factors and Ergonomics Society*, 1: 64-68.

20. Whitestone, J.J. Fabrication of Total Contact Burn Masks Employing Human Body Topography and Computer-Aided Design (CAD) and Manufacturing (CAM). *Journal of Burn Care and Rehabilitation*, publication in progress.

21. Young, S.T., Yip, S.W., Cheng, H.C., and Shieh, D.B., (1994). Three Dimensional Surface Digitizer for Facial Contour Capture. *IEEE Engineering in Medicine and Biology*, 13(1): 125-128.

APPENDIX A

IDEAL HEAD SCAN WITH EACH OF THE 17 IMPULSE SEQUENCES ADDED SEPARATELY

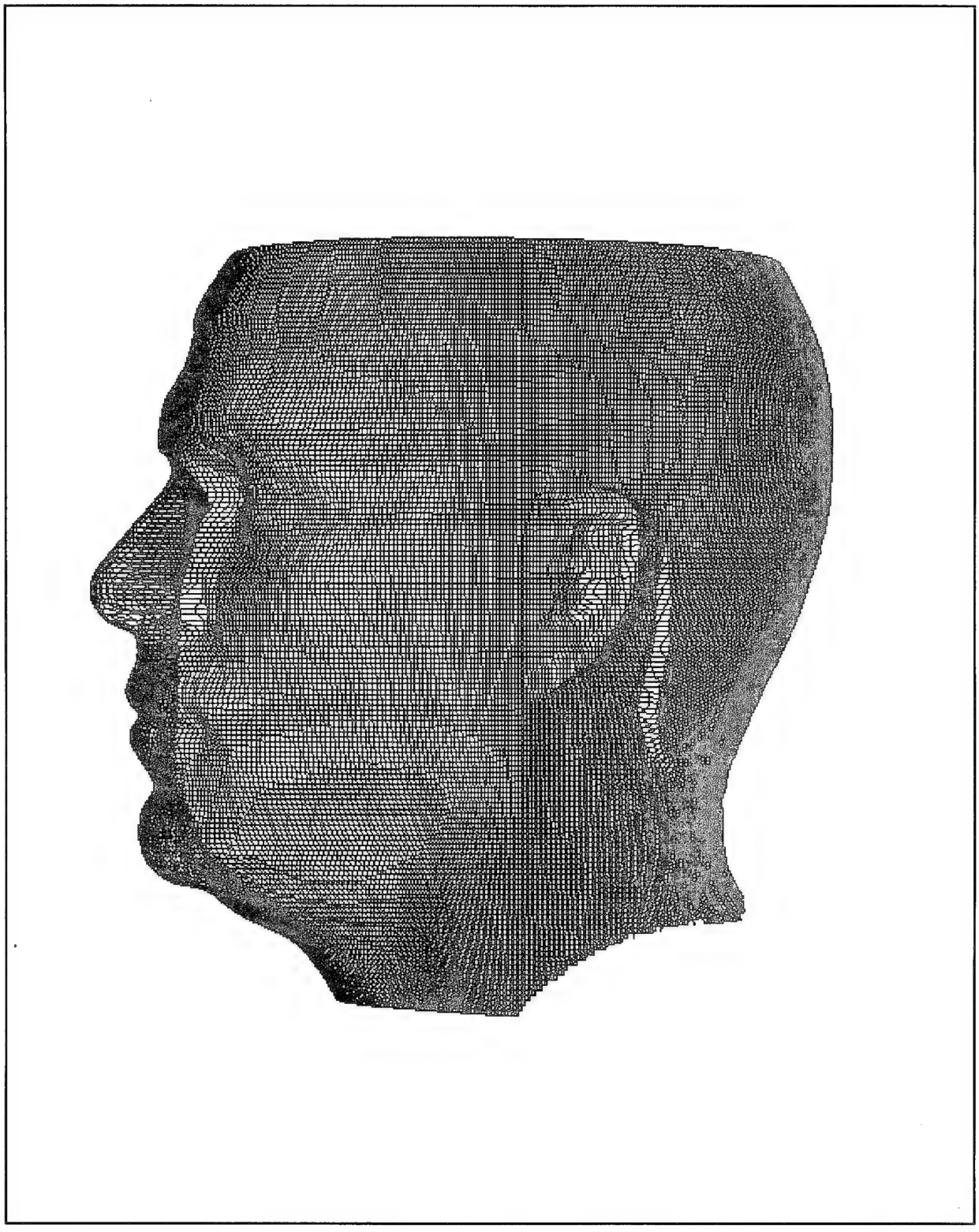

FIGURE A-1. Ideal Head Scan

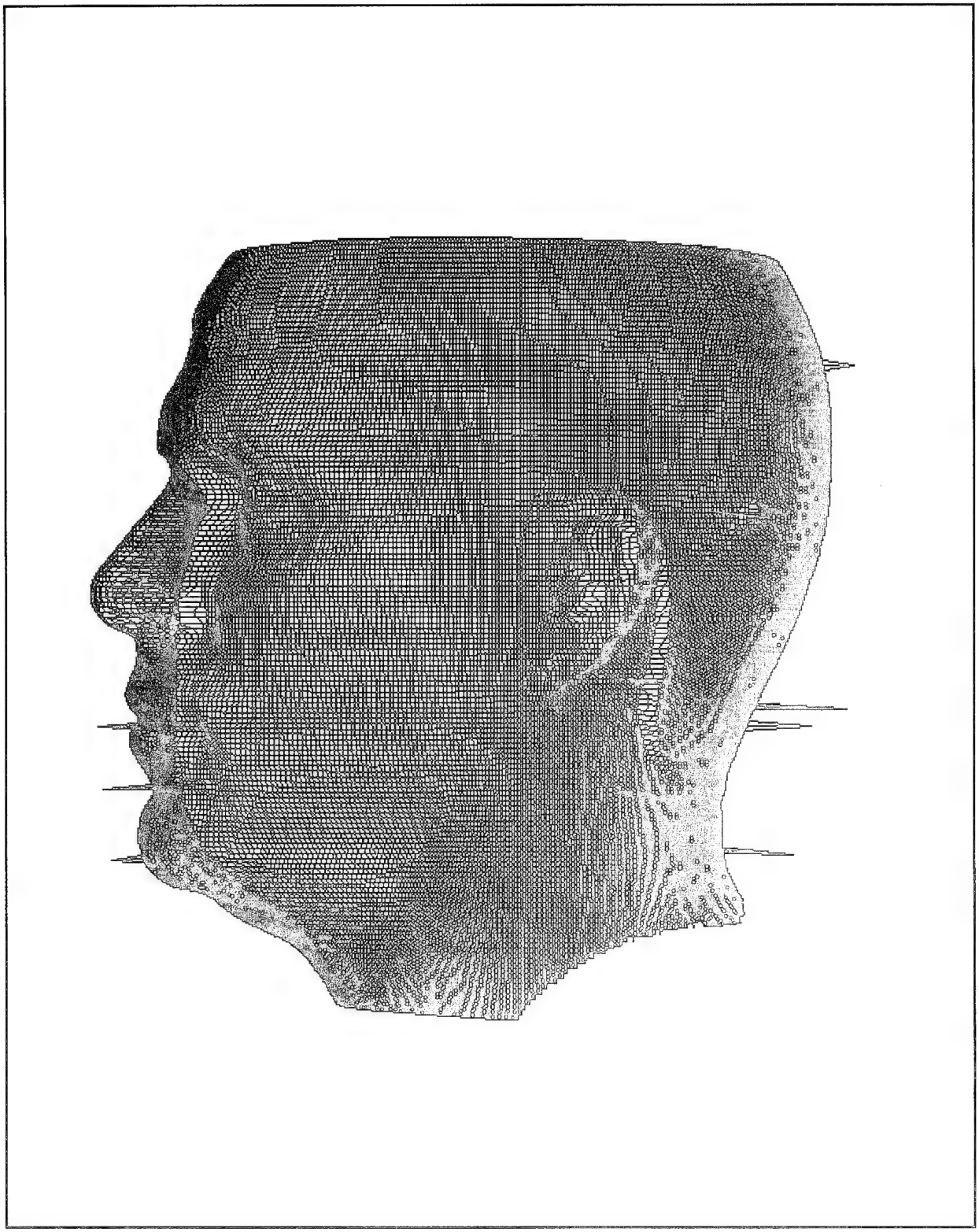

FIGURE A-2. Good Scan Plus Spike Sequence 1 (35 Spikes)

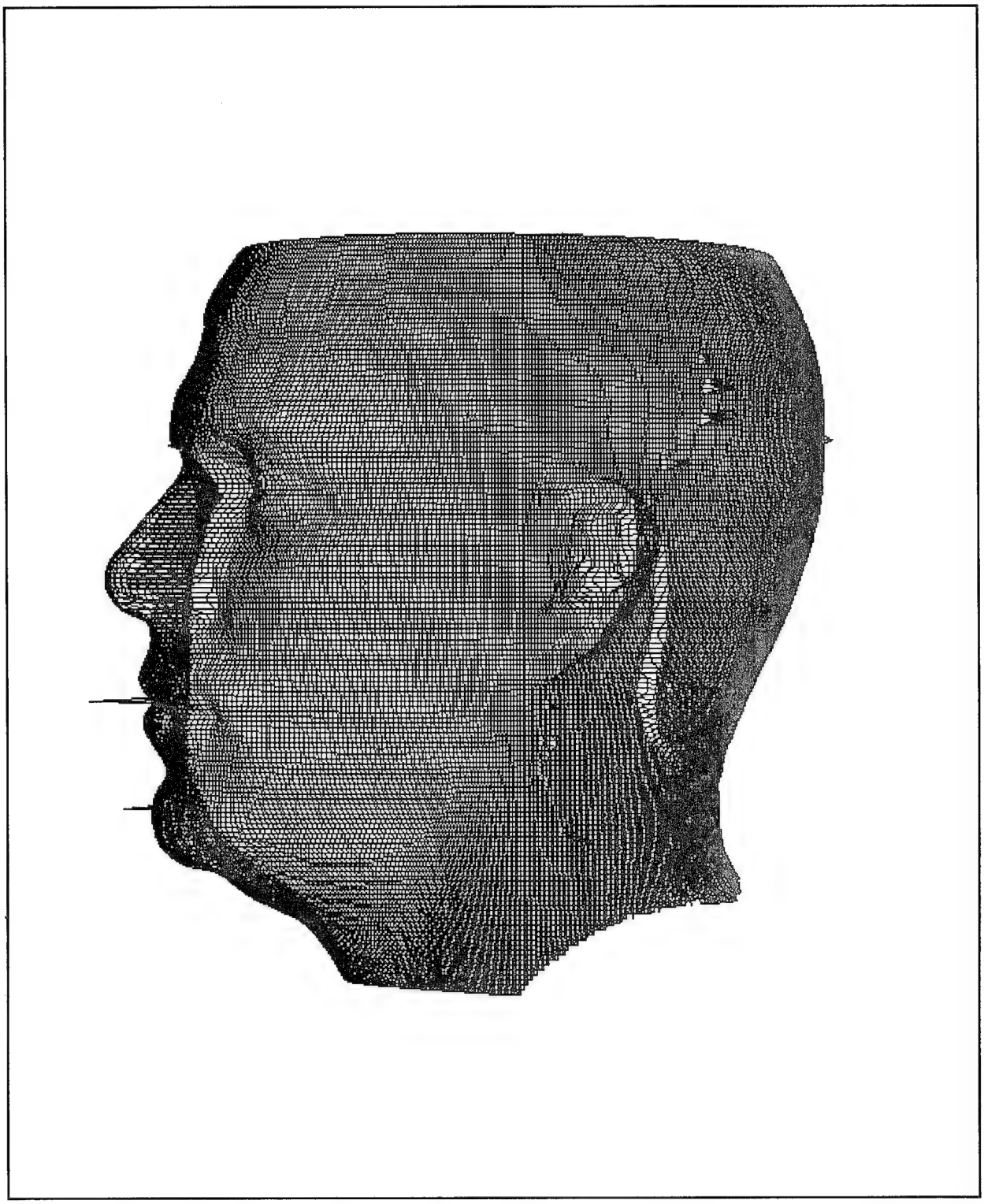

FIGURE A-3. Good Scan Plus Spike Sequence 2 (69 Spikes)

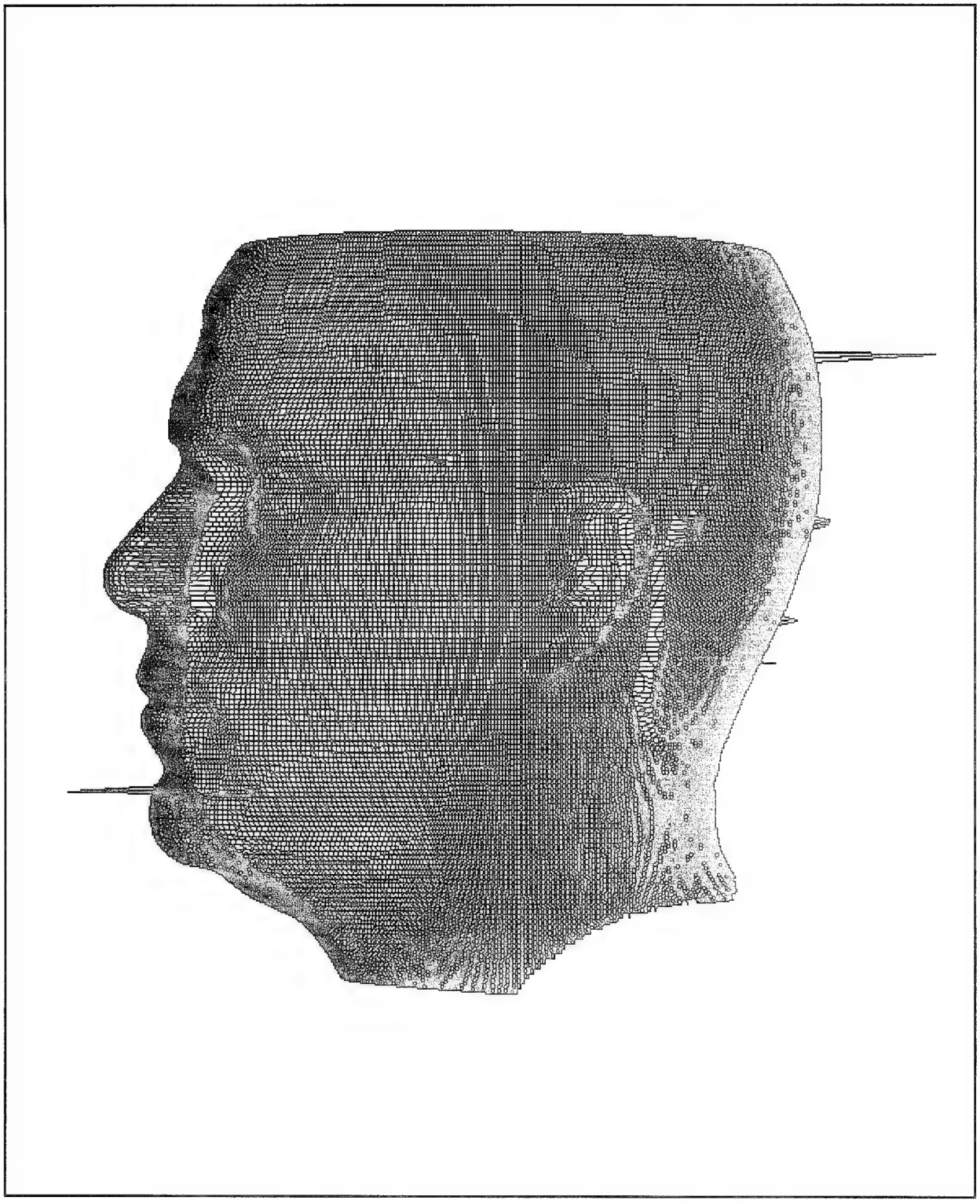

FIGURE A-4. Good Scan Plus Spike Sequence 3 (57 Spikes)

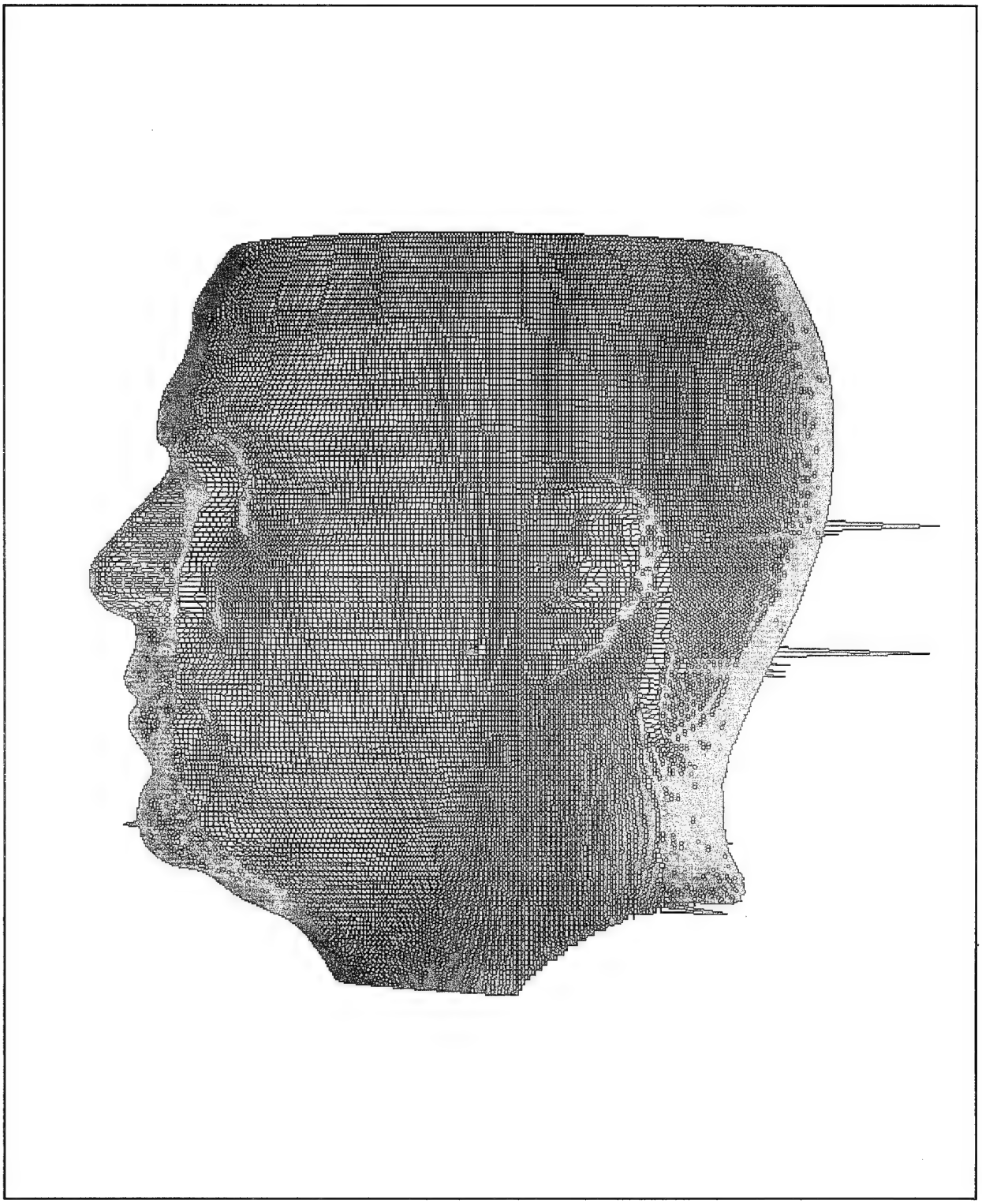

FIGURE A-5. Good Scan Plus Spike Sequence 4 (51 Spikes)

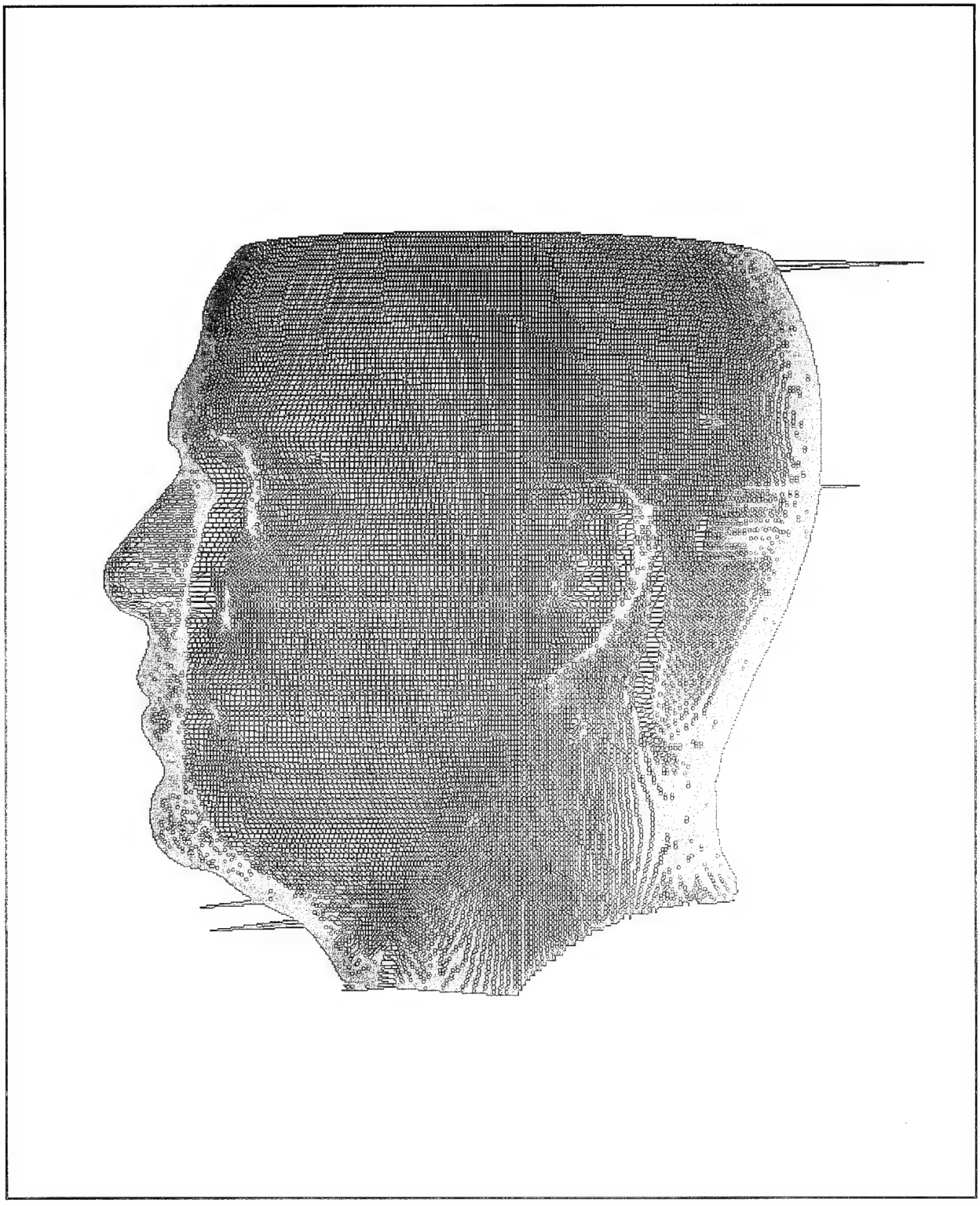

FIGURE A-6. Good Scan Plus Spike Sequence 5 (113 Spikes)

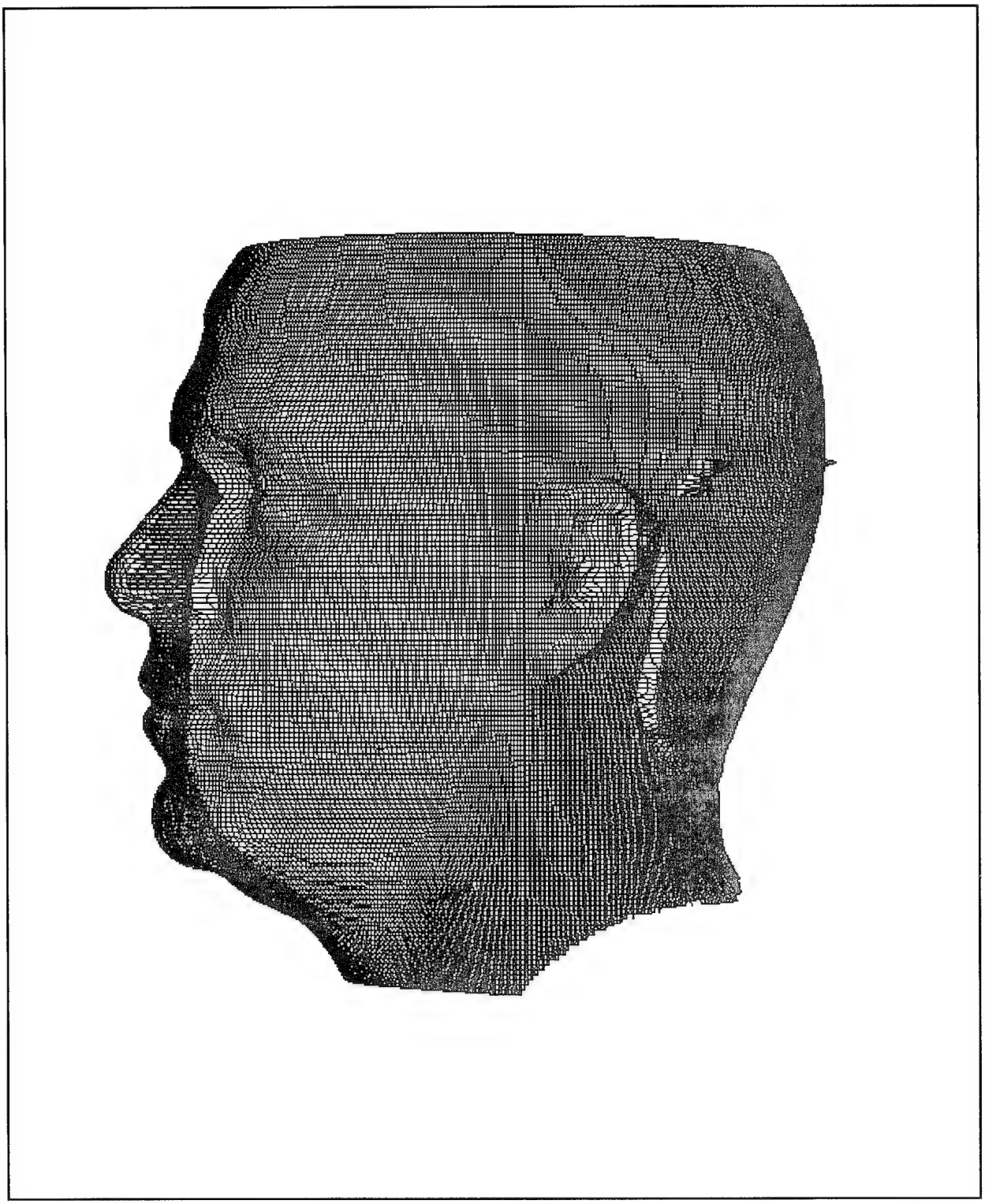

FIGURE A-7. Good Scan Plus Spike Sequence 6 (50 Spikes)

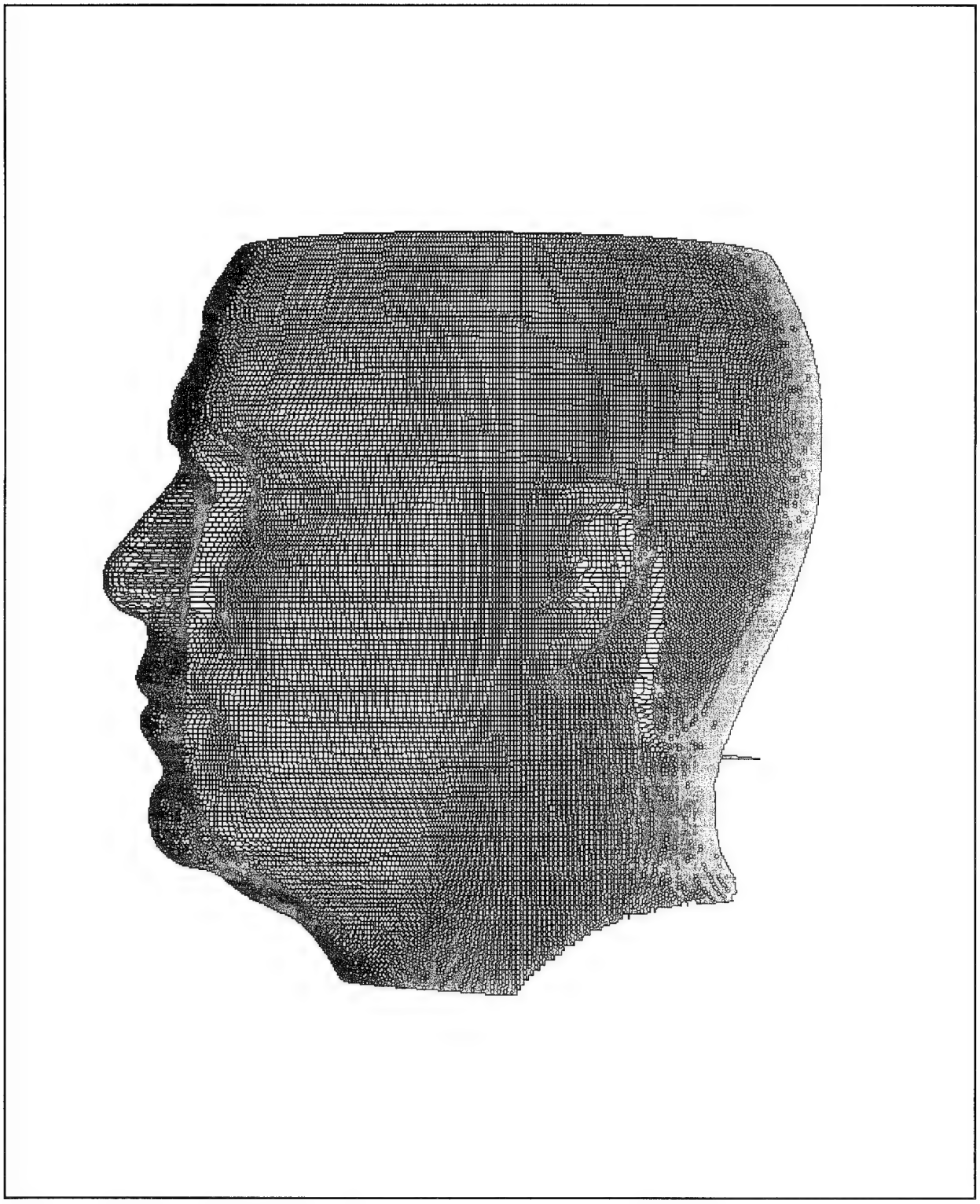

FIGURE A-8. Good Scan Plus Spike Sequence 7 (69 Spikes)

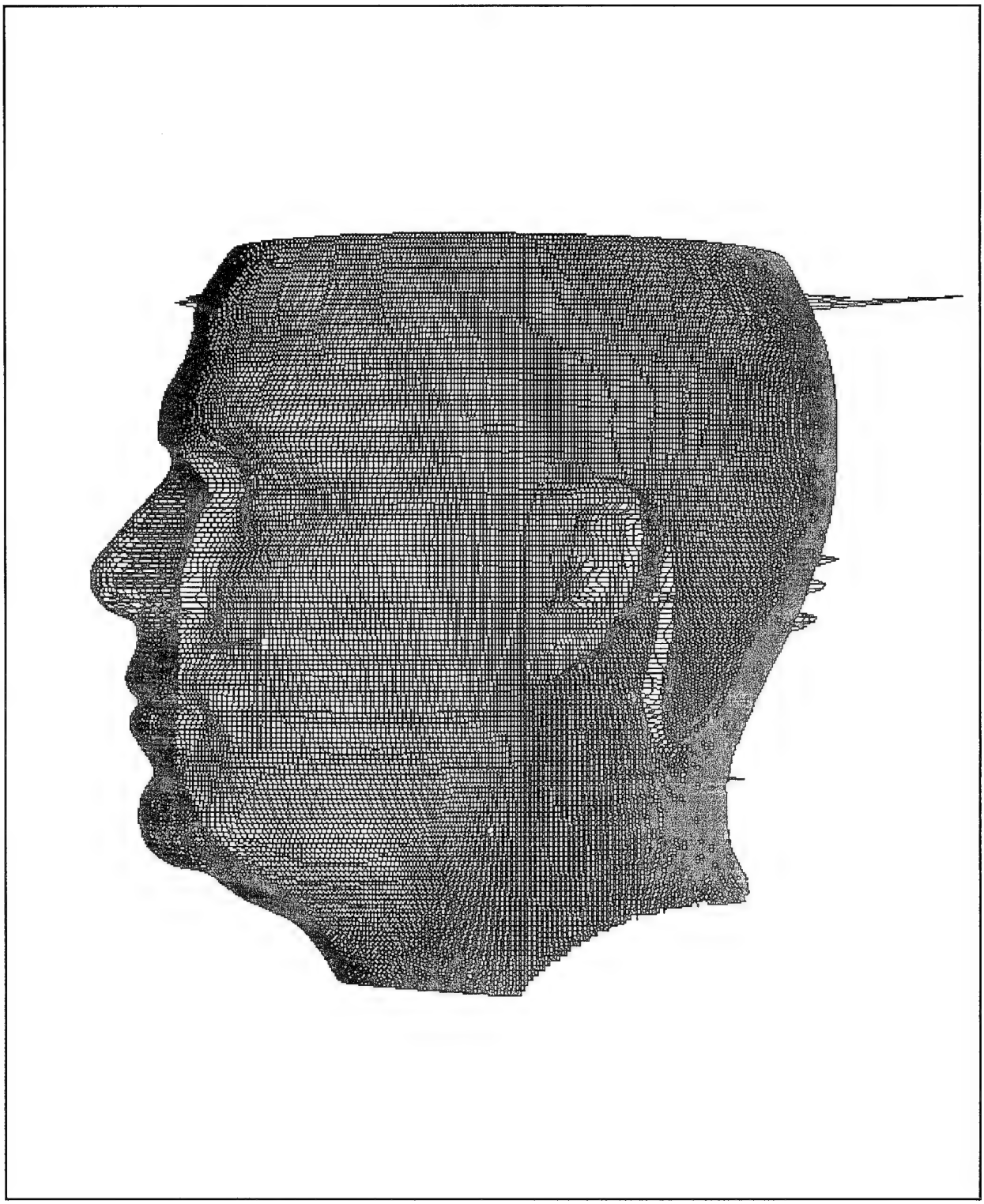

FIGURE A-9. Good Scan Plus Spike Sequence 8 (35 Spikes)

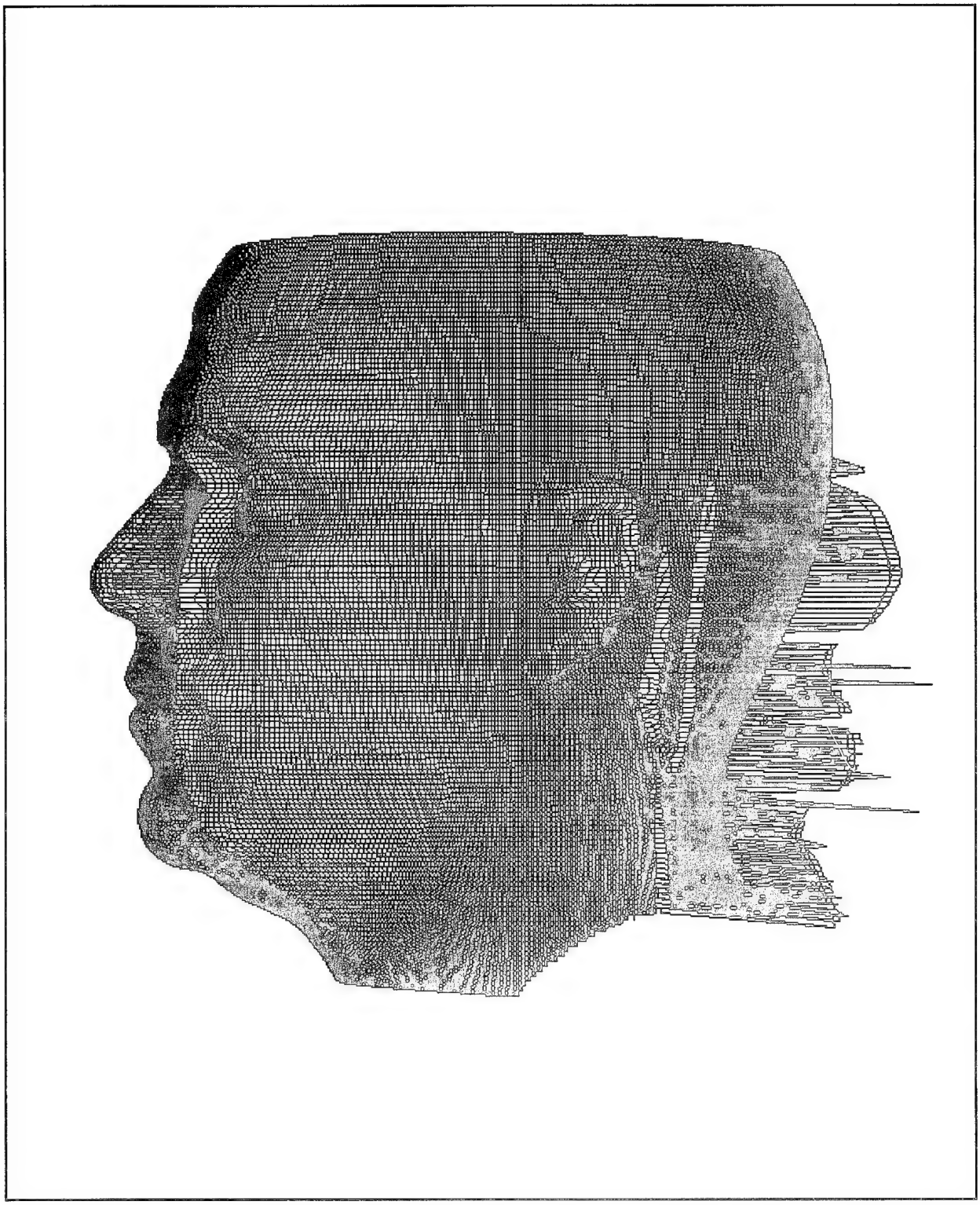

FIGURE A-10. Good Scan Plus Spike Sequence 9 (818 Spikes)

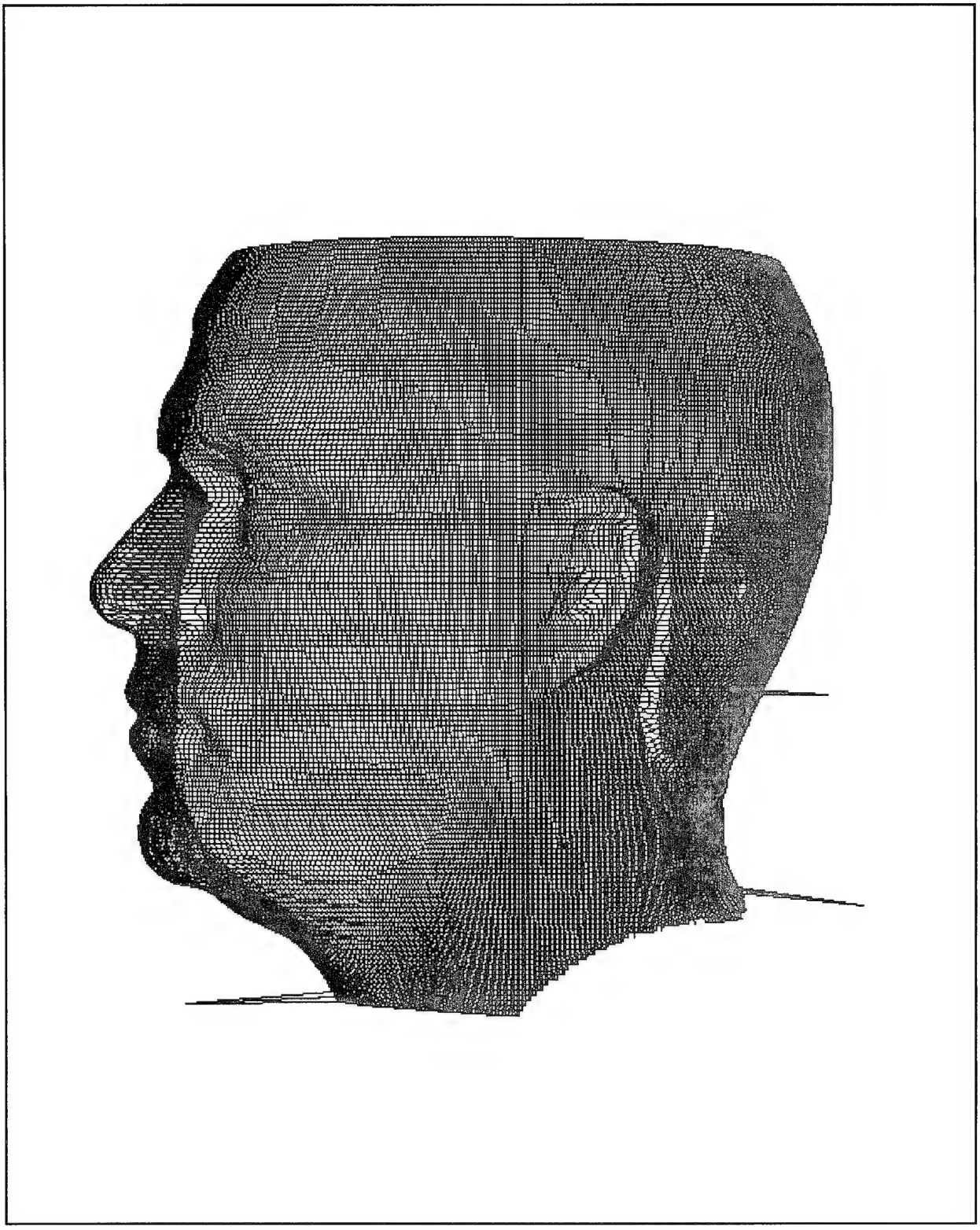

FIGURE A-11. Good Scan Plus Spike Sequence 10 (110 Spikes)

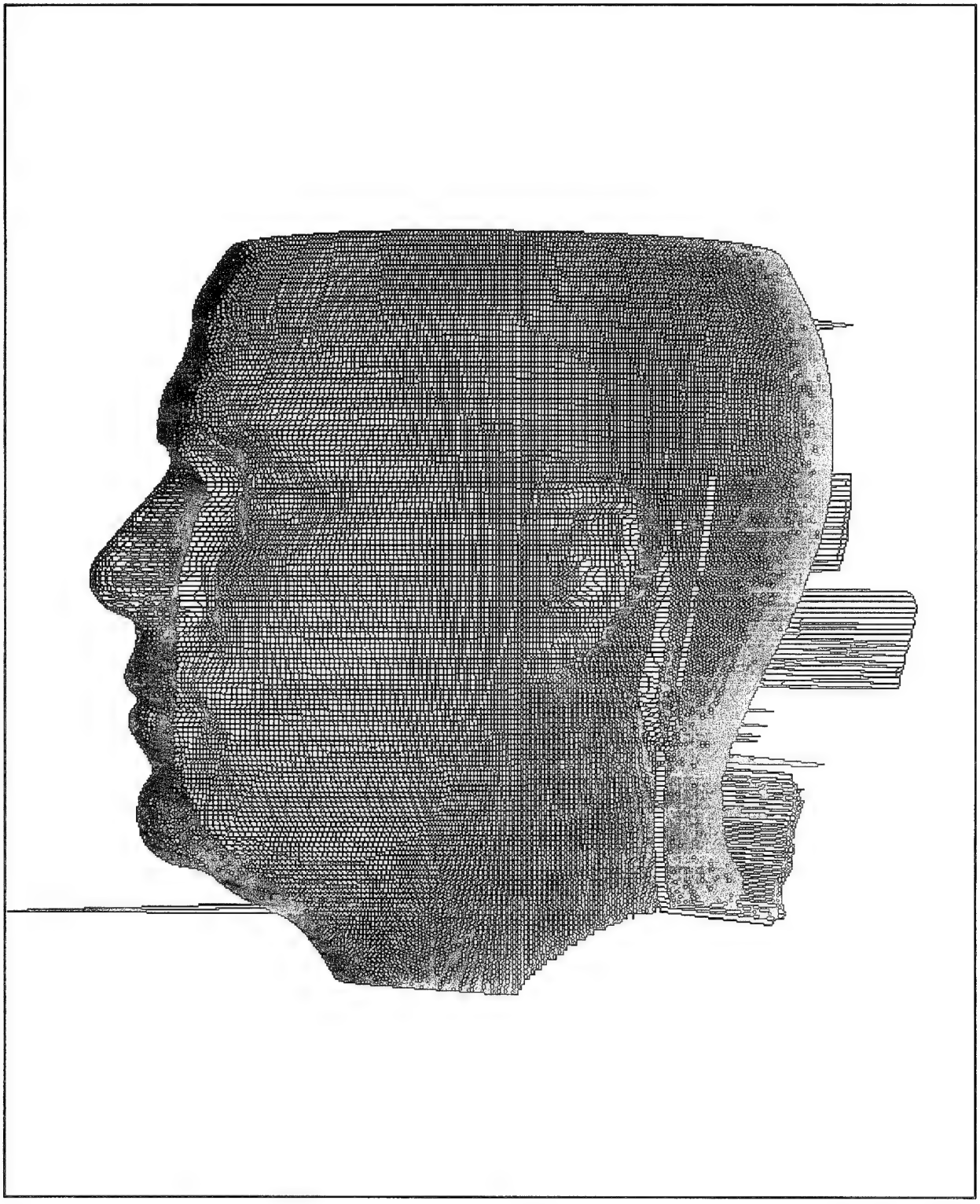

FIGURE A-12. Good Scan Plus Spike Sequence 11 (491 Spikes)

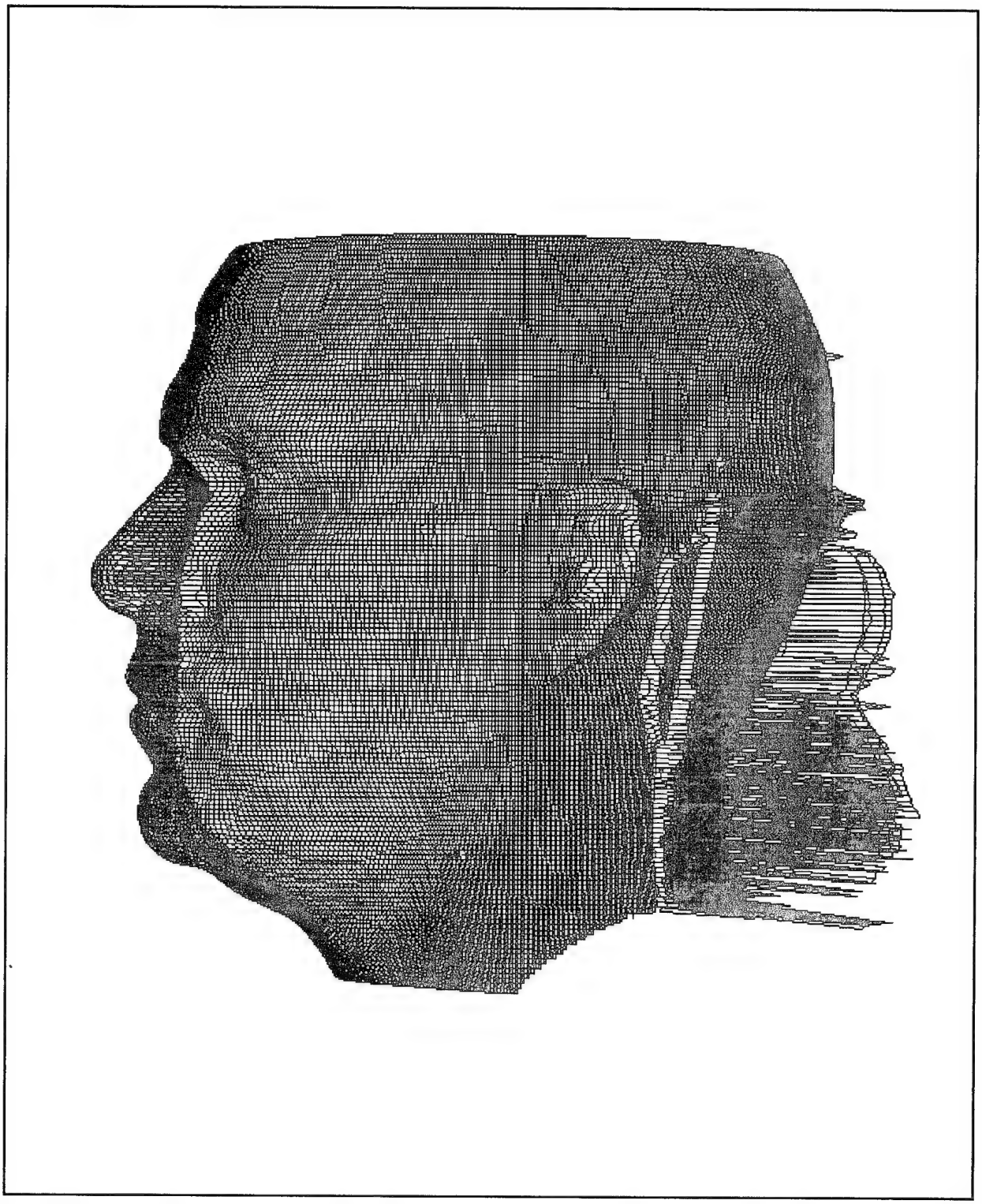

FIGURE A-13. Good Scan Plus Spike Sequence 12 (935 Spikes)

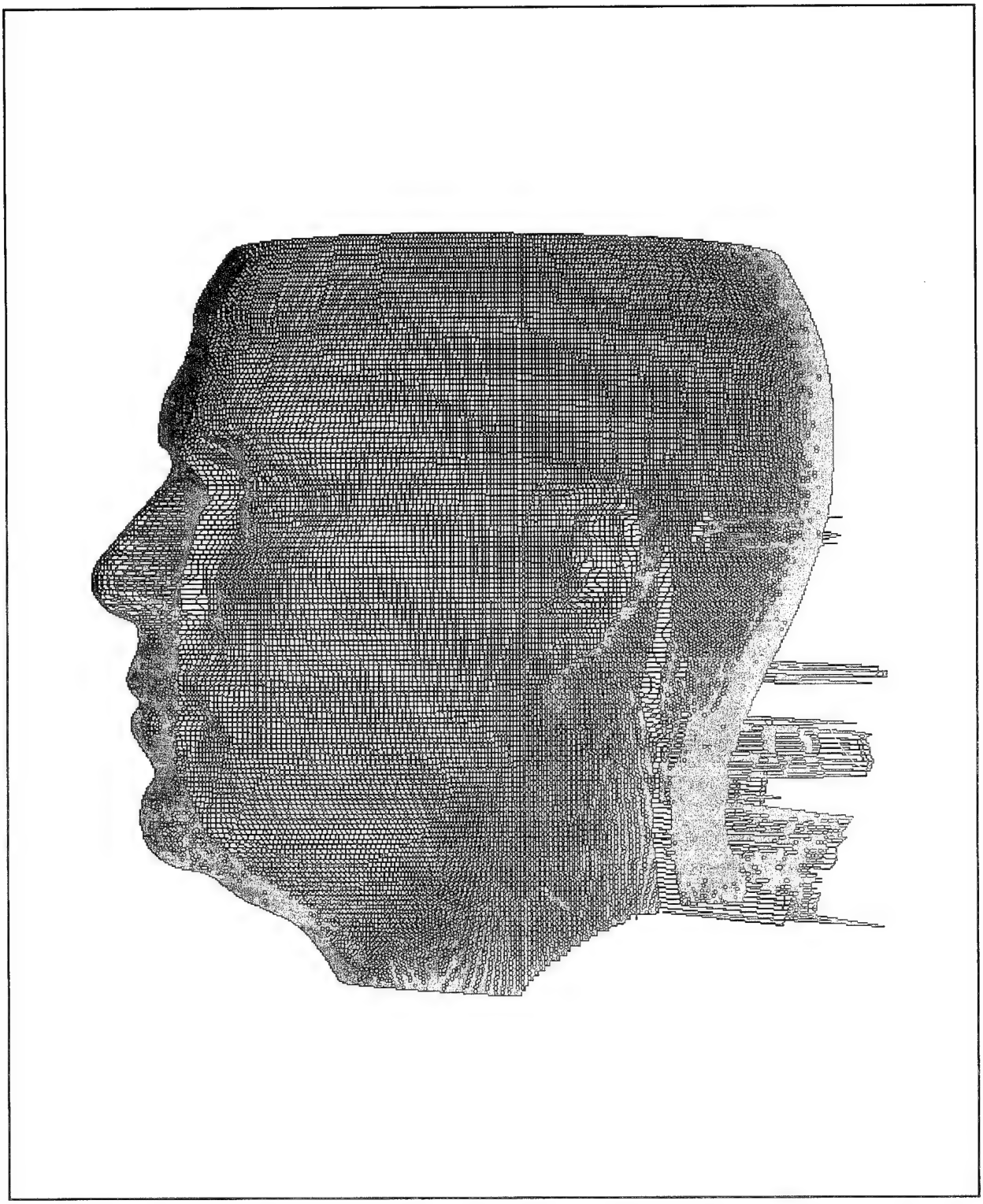

FIGURE A-14. Good Scan Plus Spike Sequence 13 (803 Spikes)

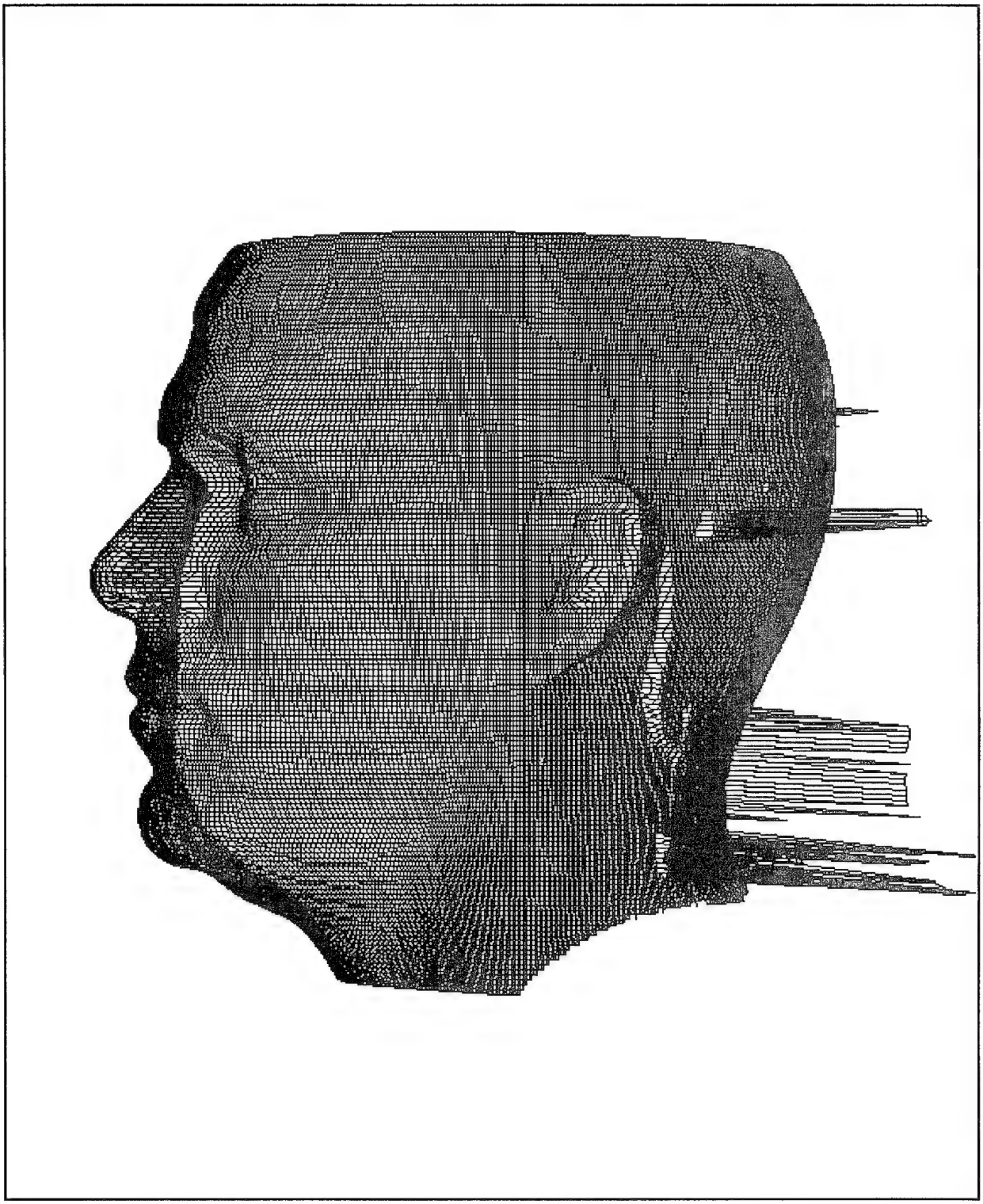

FIGURE A-15. Good Scan Plus Spike Sequence 14 (118 Spikes)

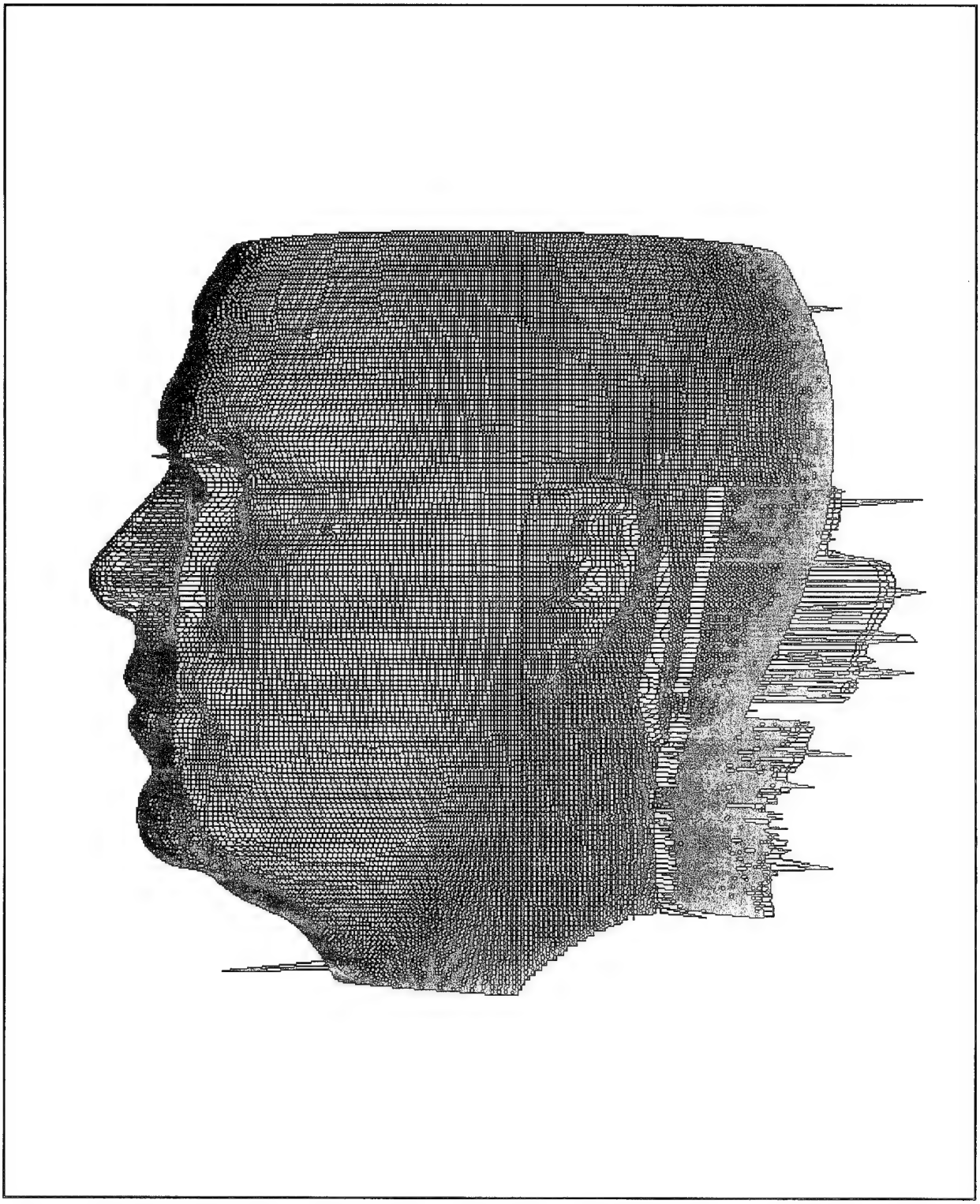

FIGURE A-16. Good Scan Plus Spike Sequence 15 (983 Spikes)

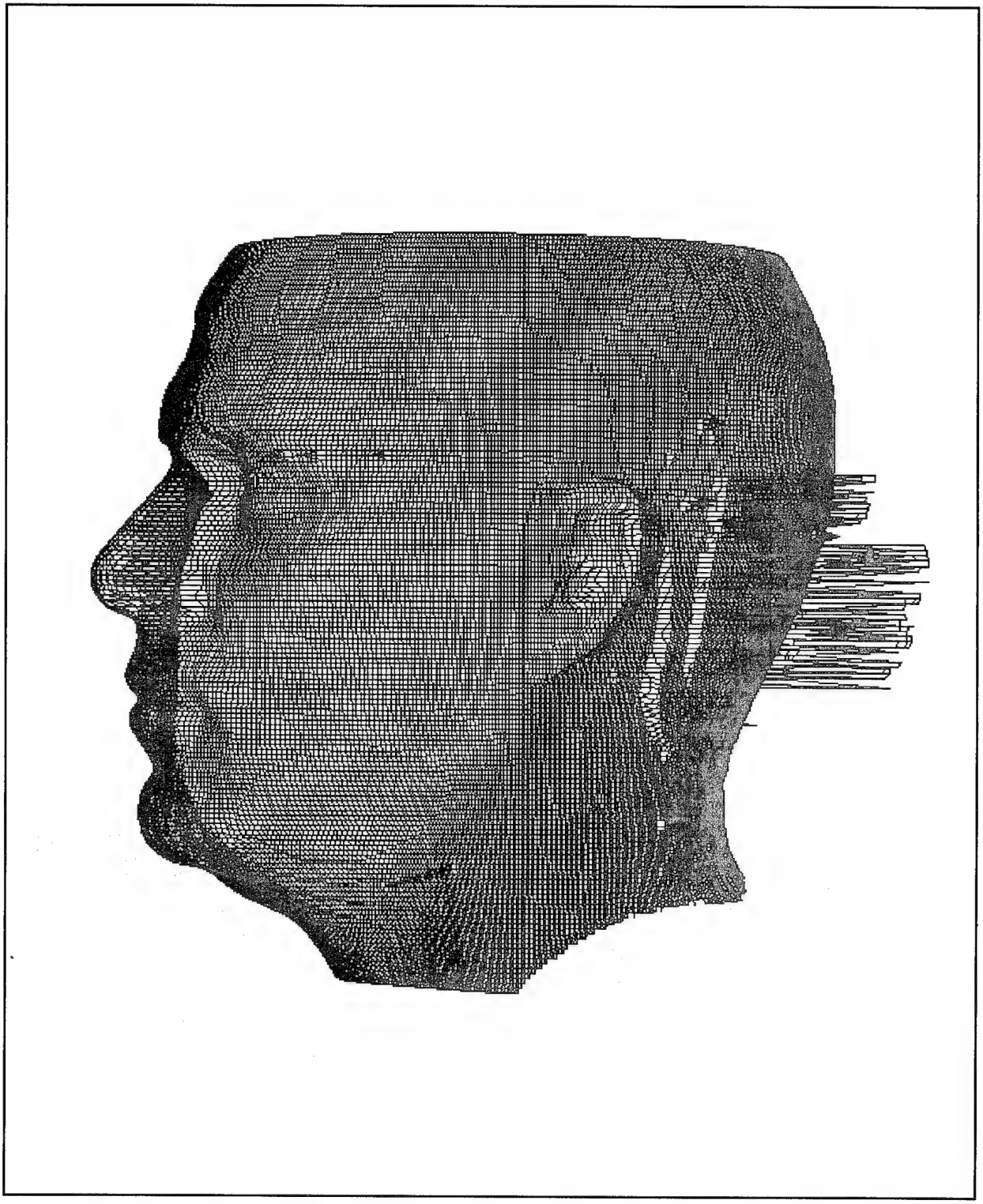

FIGURE A-17. Good Scan Plus Spike Sequence 16 (197 Spikes)

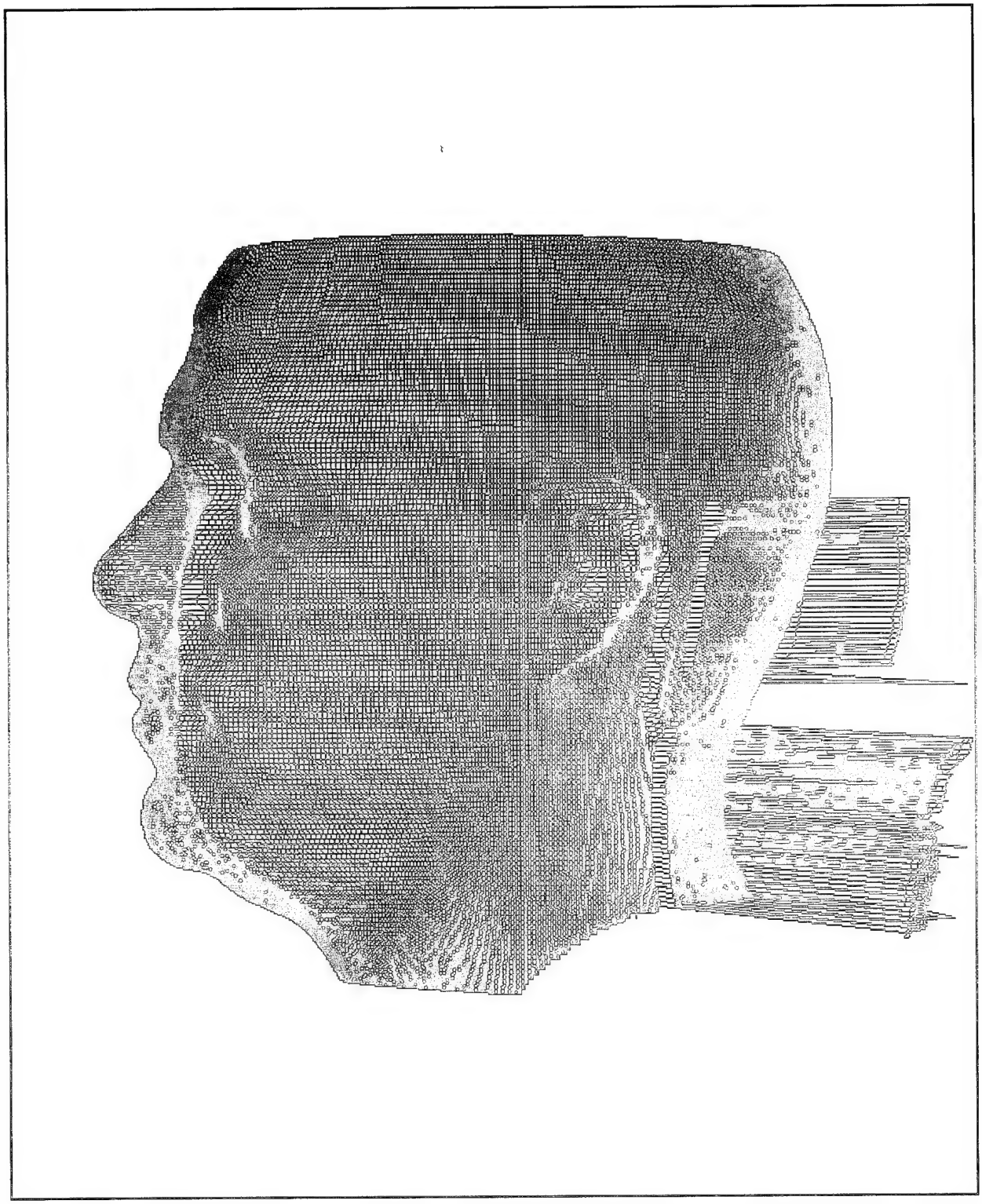

FIGURE A-18. Good Scan Plus Spike Sequence 17 (930 Spikes)

APPENDIX B

TABLES CONTAINING RESULTS OF VARIOUS OPENING SIZES

TABLE B-1.
OPERATION: OPENING OF SIZE 1.5

HEAD SCAN 105			
	Spikes		1mm Accuracy
	Identified	Corrected	Other Points Moved
Entire Head	78.9% [σ: 13.86 (17)]	60.1% [σ: 23.01 (17)]	0.3% [σ: 0.00 (17)]
Back of Head	80.3% [σ: 14.51 (17)]	61.7% [σ: 24.59 (17)]	0.0% [σ: 0.00 (17)]
Ears	85.7% [σ: 28.57 (4)]	82.1% [σ: 35.72 (4)]	1.9% [σ: 0.01 (17)]
Eyes	89.1% [σ: 15.46 (2)]	78.1% [σ: 30.94 (2)]	0.1% [σ: 0.00 (17)]
Nose	0.0% [σ: 0.00 (1)]	0.0% [σ: 0.00 (1)]	1.5% [σ: 0.00 (17)]
HEAD SCAN 177			
	Spikes		1mm Accuracy
	Identified	Corrected	Other Points Moved
Entire Head	77.0% [σ: 16.08 (17)]	54.3% [σ: 24.95 (17)]	0.8% [σ: 0.00 (17)]
Back of Head	77.9% [σ: 16.64 (17)]	54.4% [σ: 24.27 (17)]	1.1% [σ: 0.01 (17)]
Ears	87.5% [σ: 25.00 (4)]	75.0% [σ: 50.00 (4)]	1.9% [σ: 0.01 (17)]
Eyes	93.3% [σ: 11.55 (3)]	82.7% [σ: 30.02 (3)]	4.1% [σ: 0.00 (17)]
Nose	100.0% [σ: 0.00 (2)]	100.0% [σ: 0.00 (2)]	0.9% [σ: 0.00 (17)]
HEAD SCAN 334			
	Spikes		1mm Accuracy
	Identified	Corrected	Other Points Moved
Entire Head	81.2% [σ: 13.40 (17)]	62.0% [σ: 21.31 (17)]	0.2% [σ: 0.00 (17)]
Back of Head	82.6% [σ: 13.05 (17)]	64.7% [σ: 22.93 (17)]	0.0% [σ: 0.00 (17)]
Ears	81.3% [σ: 27.24 (5)]	54.0% [σ: 45.61 (5)]	2.1% [σ: 0.00 (17)]
Eyes	89.4% [σ: 18.37 (3)]	84.9% [σ: 26.24 (3)]	1.6% [σ: 0.00 (17)]
Nose	0.0% [σ: 0.00 (1)]	0.0% [σ: 0.00 (1)]	2.0% [σ: 0.00 (17)]
HEAD SCAN 356			
	Spikes		1mm Accuracy
	Identified	Corrected	Other Points Moved
Entire Head	77.4% [σ: 14.09 (17)]	57.6% [σ: 24.04 (17)]	0.2% [σ: 0.00 (17)]
Back of Head	75.8% [σ: 16.75 (17)]	55.5% [σ: 26.08 (17)]	0.1% [σ: 0.00 (17)]
Ears	91.7% [σ: 14.43 (3)]	58.3% [σ: 38.19 (3)]	0.6% [σ: 0.01 (17)]
Eyes	100.0% [σ: 0.00 (2)]	100.0% [σ: 0.00 (2)]	1.6% [σ: 0.00 (17)]
Nose	81.0% [σ: 32.99 (3)]	71.4% [σ: 49.48 (3)]	2.6% [σ: 0.00 (17)]
HEAD SCAN DAN1			
	Spikes		1mm Accuracy
	Identified	Corrected	Other Points Moved
Entire Head	72.0% [σ: 16.58 (17)]	51.8% [σ: 25.85 (17)]	0.1% [σ: 0.00 (17)]
Back of Head	75.2% [σ: 16.69 (17)]	55.0% [σ: 26.81 (17)]	0.0% [σ: 0.00 (17)]
Ears	99.0% [σ: 3.35 (11)]	72.7% [σ: 35.18 (11)]	0.7% [σ: 0.01 (17)]
Eyes	100.0% [σ: 0.00 (3)]	91.7% [σ: 14.43 (3)]	2.7% [σ: 0.00 (17)]
Nose	100.0% [σ: 0.00 (1)]	100.0% [σ: 0.00 (1)]	3.1% [σ: 0.00 (17)]

TABLE B-2.
OPERATION: OPENING OF SIZE 2.0

HEAD SCAN 105			
	Spikes		1mm Accuracy
	Identified	Corrected	Other Points Moved
Entire Head	93.3% [σ: 7.42 (17)]	73.7% [σ: 20.87 (17)]	0.6% [σ: 0.00 (17)]
Back of Head	93.1% [σ: 7.86 (17)]	74.5% [σ: 22.32 (17)]	0.1% [σ: 0.00 (17)]
Ears	100.0% [σ: 0.00 (4)]	100.0% [σ: 0.00 (4)]	3.1% [σ: 0.00 (17)]
Eyes	100.0% [σ: 0.00 (2)]	95.3% [σ: 6.63 (2)]	0.3% [σ: 0.02 (17)]
Nose	100.0% [σ: 0.00 (1)]	100.0% [σ: 0.00 (1)]	0.2% [σ: 0.00 (17)]
HEAD SCAN 177			
	Spikes		1mm Accuracy
	Identified	Corrected	Other Points Moved
Entire Head	91.4% [σ: 8.64 (17)]	68.0% [σ: 23.45 (17)]	1.6% [σ: 0.01 (17)]
Back of Head	91.0% [σ: 9.48 (17)]	67.2% [σ: 25.10 (17)]	2.0% [σ: 0.01 (17)]
Ears	100.0% [σ: 0.00 (4)]	62.5% [σ: 47.87 (4)]	6.0% [σ: 0.01 (17)]
Eyes	100.0% [σ: 0.00 (3)]	96.0% [σ: 6.93 (3)]	8.0% [σ: 0.12 (17)]
Nose	100.0% [σ: 0.00 (2)]	50.0% [σ: 70.71 (2)]	1.5% [σ: 0.00 (17)]
HEAD SCAN 334			
	Spikes		1mm Accuracy
	Identified	Corrected	Other Points Moved
Entire Head	95.5% [σ: 4.38 (17)]	80.2% [σ: 17.26 (17)]	0.5% [σ: 0.00 (17)]
Back of Head	95.8% [σ: 4.43 (17)]	82.1% [σ: 17.68 (17)]	0.0% [σ: 0.00 (17)]
Ears	96.0% [σ: 8.94 (5)]	96.0% [σ: 8.94 (5)]	4.4% [σ: 0.01 (17)]
Eyes	98.5% [σ: 2.63 (3)]	100.0% [σ: 0.00 (3)]	2.5% [σ: 0.00 (17)]
Nose	100.0% [σ: 0.00 (1)]	100.0% [σ: 0.00 (1)]	1.3% [σ: 0.00 (17)]
HEAD SCAN 356			
	Spikes		1mm Accuracy
	Identified	Corrected	Other Points Moved
Entire Head	89.9% [σ: 8.66 (17)]	67.3% [σ: 23.15 (17)]	0.4% [σ: 0.00 (17)]
Back of Head	87.5% [σ: 10.87 (17)]	64.9% [σ: 27.42 (17)]	0.0% [σ: 0.00 (17)]
Ears	91.7% [σ: 14.43 (3)]	75.0% [σ: 25.00 (3)]	2.4% [σ: 0.00 (17)]
Eyes	100.0% [σ: 0.00 (2)]	100.0% [σ: 0.00 (2)]	4.0% [σ: 0.00 (17)]
Nose	90.5% [σ: 16.49 (3)]	76.2% [σ: 41.24 (3)]	1.5% [σ: 0.00 (17)]
HEAD SCAN DAN1			
	Spikes		1mm Accuracy
	Identified	Corrected	Other Points Moved
Entire Head	90.6% [σ: 10.16 (17)]	69.2% [σ: 25.10 (17)]	0.2% [σ: 0.00 (17)]
Back of Head	91.1% [σ: 10.17 (17)]	68.5% [σ: 26.06 (17)]	0.0% [σ: 0.00 (17)]
Ears	100.0% [σ: 0.00 (11)]	89.9% [σ: 30.00 (11)]	3.0% [σ: 0.01 (17)]
Eyes	100.0% [σ: 0.00 (3)]	75.0% [σ: 43.30 (3)]	3.7% [σ: 0.10 (17)]
Nose	100.0% [σ: 0.00 (1)]	100.0% [σ: 0.00 (1)]	0.7% [σ: 0.00 (17)]

TABLE B-3.
OPERATION: OPENING OF SIZE 2.5

HEAD SCAN 105

	Spikes		1mm Accuracy
	Identified	Corrected	Other Points Moved
Entire Head	97.1% [σ: 3.71 (17)]	82.1% [σ: 15.16 (17)]	0.8% [σ: 0.00 (17)]
Back of Head	96.8% [σ: 3.91 (17)]	82.6% [σ: 17.01 (17)]	0.1% [σ: 0.00 (17)]
Ears	100.0% [σ: 0.00 (4)]	100.0% [σ: 0.00 (4)]	4.9% [σ: 0.00 (17)]
Eyes	100.0% [σ: 0.00 (2)]	96.9% [σ: 4.42 (2)]	0.8% [σ: 0.00 (17)]
Nose	100.0% [σ: 0.00 (1)]	100.0% [σ: 0.00 (1)]	0.6% [σ: 0.00 (17)]

HEAD SCAN 177

	Spikes		1mm Accuracy
	Identified	Corrected	Other Points Moved
Entire Head	96.4% [σ: 3.96 (17)]	77.3% [σ: 18.39 (17)]	2.1% [σ: 0.01 (17)]
Back of Head	95.8% [σ: 4.42 (17)]	75.6% [σ: 21.29 (17)]	2.7% [σ: 0.02 (17)]
Ears	100.0% [σ: 0.00 (4)]	62.5% [σ: 47.87 (4)]	7.8% [σ: 0.01 (17)]
Eyes	98.7% [σ: 2.31 (3)]	94.7% [σ: 9.24 (3)]	10.5% [σ: 0.19 (17)]
Nose	100.0% [σ: 0.00 (2)]	100.0% [σ: 0.00 (2)]	2.2% [σ: 0.00 (17)]

HEAD SCAN 334

	Spikes		1mm Accuracy
	Identified	Corrected	Other Points Moved
Entire Head	97.3% [σ: 3.81 (17)]	85.0% [σ: 14.36 (17)]	0.6% [σ: 0.00 (17)]
Back of Head	97.7% [σ: 3.69 (17)]	87.7% [σ: 13.72 (17)]	0.0% [σ: 0.00 (17)]
Ears	96.0% [σ: 8.94 (5)]	89.3% [σ: 15.35 (5)]	6.0% [σ: 0.01 (17)]
Eyes	100.0% [σ: 0.00 (3)]	100.0% [σ: 0.00 (3)]	4.1% [σ: 0.00 (17)]
Nose	100.0% [σ: 0.00 (1)]	100.0% [σ: 0.00 (1)]	1.3% [σ: 0.00 (17)]

HEAD SCAN 356

	Spikes		1mm Accuracy
	Identified	Corrected	Other Points Moved
Entire Head	94.7% [σ: 5.50 (17)]	76.5% [σ: 20.21 (17)]	0.6% [σ: 0.00 (17)]
Back of Head	93.6% [σ: 7.03 (17)]	73.6% [σ: 26.20 (17)]	0.1% [σ: 0.00 (17)]
Ears	100.0% [σ: 0.00 (3)]	75.0% [σ: 25.00 (3)]	5.8% [σ: 0.05 (17)]
Eyes	100.0% [σ: 0.00 (2)]	100.0% [σ: 0.00 (2)]	4.2% [σ: 0.00 (17)]
Nose	90.5% [σ: 16.49 (3)]	76.2% [σ: 41.24 (3)]	3.3% [σ: 0.00 (17)]

HEAD SCAN DAN1

	Spikes		1mm Accuracy
	Identified	Corrected	Other Points Moved
Entire Head	94.8% [σ: 6.52 (17)]	76.1% [σ: 22.66 (17)]	0.3% [σ: 0.00 (17)]
Back of Head	95.0% [σ: 6.59 (17)]	77.1% [σ: 23.56 (17)]	0.0% [σ: 0.00 (17)]
Ears	100.0% [σ: 0.00 (11)]	78.8% [σ: 33.41 (11)]	4.7% [σ: 0.01 (17)]
Eyes	100.0% [σ: 0.00 (3)]	100.0% [σ: 0.00 (3)]	4.3% [σ: 0.00 (17)]
Nose	100.0% [σ: 0.00 (1)]	100.0% [σ: 0.00 (1)]	0.3% [σ: 0.00 (17)]

TABLE B-4.
OPERATION: OPENING OF SIZE 3.0

HEAD SCAN 105			
	Spikes		1mm Accuracy
	Identified	Corrected	Other Points Moved
Entire Head	98.5% [σ: 3.15 (17)]	88.5% [σ: 12.19 (17)]	1.3% [σ: 0.00 (17)]
Back of Head	98.4% [σ: 3.29 (17)]	88.2% [σ: 13.83 (17)]	0.1% [σ: 0.00 (17)]
Ears	100.0% [σ: 0.00 (4)]	100.0% [σ: 0.00 (4)]	11.1% [σ: 0.00 (17)]
Eyes	100.0% [σ: 0.00 (2)]	96.9% [σ: 4.42 (2)]	0.9% [σ: 0.00 (17)]
Nose	100.0% [σ: 0.00 (1)]	100.0% [σ: 0.00 (1)]	1.5% [σ: 0.00 (17)]
HEAD SCAN 177			
	Spikes		1mm Accuracy
	Identified	Corrected	Other Points Moved
Entire Head	98.1% [σ: 3.03 (17)]	83.5% [σ: 15.52 (17)]	2.6% [σ: 0.01 (17)]
Back of Head	97.7% [σ: 3.27 (17)]	81.6% [σ: 18.08 (17)]	3.1% [σ: 0.02 (17)]
Ears	100.0% [σ: 0.00 (4)]	62.5% [σ: 47.87 (4)]	11.4% [σ: 0.01 (17)]
Eyes	98.7% [σ: 2.31 (3)]	93.3% [σ: 11.55 (3)]	12.5% [σ: 0.19 (17)]
Nose	100.0% [σ: 0.00 (2)]	100.0% [σ: 0.00 (2)]	2.1% [σ: 0.00 (17)]
HEAD SCAN 334			
	Spikes		1mm Accuracy
	Identified	Corrected	Other Points Moved
Entire Head	99.8% [σ: 0.49 (17)]	91.8% [σ: 9.16 (17)]	1.0% [σ: 0.00 (17)]
Back of Head	99.7% [σ: 0.76 (17)]	93.4% [σ: 8.55 (17)]	0.0% [σ: 0.00 (17)]
Ears	100.0% [σ: 0.00 (5)]	86.7% [σ: 29.82 (5)]	13.1% [σ: 0.05 (17)]
Eyes	100.0% [σ: 0.00 (3)]	100.0% [σ: 0.00 (3)]	4.8% [σ: 0.00 (17)]
Nose	100.0% [σ: 0.00 (1)]	100.0% [σ: 0.00 (1)]	1.8% [σ: 0.00 (17)]
HEAD SCAN 356			
	Spikes		1mm Accuracy
	Identified	Corrected	Other Points Moved
Entire Head	97.1% [σ: 3.90 (17)]	81.4% [σ: 17.50 (17)]	0.9% [σ: 0.00 (17)]
Back of Head	96.5% [σ: 4.34 (17)]	78.0% [σ: 23.55 (17)]	0.1% [σ: 0.00 (17)]
Ears	100.0% [σ: 0.00 (3)]	58.3% [σ: 52.04 (3)]	9.3% [σ: 0.02 (17)]
Eyes	100.0% [σ: 0.00 (2)]	100.0% [σ: 0.00 (2)]	4.8% [σ: 0.00 (17)]
Nose	90.5% [σ: 16.49 (3)]	81.0% [σ: 32.99 (3)]	4.2% [σ: 0.00 (17)]
HEAD SCAN DAN1			
	Spikes		1mm Accuracy
	Identified	Corrected	Other Points Moved
Entire Head	97.4% [σ: 4.31 (17)]	83.4% [σ: 18.49 (17)]	0.3% [σ: 0.00 (17)]
Back of Head	98.1% [σ: 3.82 (17)]	85.0% [σ: 18.94 (17)]	0.0% [σ: 0.00 (17)]
Ears	100.0% [σ: 0.00 (11)]	80.3% [σ: 35.60 (11)]	5.7% [σ: 0.01 (17)]
Eyes	100.0% [σ: 0.00 (3)]	100.0% [σ: 0.00 (3)]	4.6% [σ: 0.00 (17)]
Nose	100.0% [σ: 0.00 (1)]	100.0% [σ: 0.00 (1)]	2.0% [σ: 0.00 (17)]

TABLE B-5.
OPERATION: OPENING OF SIZE 3.5

HEAD SCAN 105			
	Spikes		1mm Accuracy
	Identified	Corrected	Other Points Moved
Entire Head	99.7% [σ: 0.92 (17)]	92.9% [σ: 8.64 (17)]	1.9% [σ: 0.14 (17)]
Back of Head	99.8% [σ: 0.67 (17)]	92.6% [σ: 9.55 (17)]	0.3% [σ: 0.05 (17)]
Ears	100.0% [σ: 0.00 (4)]	100.0% [σ: 0.00 (4)]	17.2% [σ: 1.57 (17)]
Eyes	100.0% [σ: 0.00 (2)]	96.9% [σ: 4.42 (2)]	2.2% [σ: 0.32 (17)]
Nose	100.0% [σ: 0.00 (1)]	100.0% [σ: 0.00 (1)]	3.2% [σ: 0.42 (17)]
HEAD SCAN 177			
	Spikes		1mm Accuracy
	Identified	Corrected	Other Points Moved
Entire Head	99.7% [σ: 0.98 (17)]	88.2% [σ: 10.50 (17)]	3.2% [σ: 0.16 (17)]
Back of Head	99.6% [σ: 1.30 (17)]	87.1% [σ: 11.90 (17)]	3.6% [σ: 0.11 (17)]
Ears	100.0% [σ: 0.00 (4)]	62.5% [σ: 47.87 (4)]	18.7% [σ: 1.89 (17)]
Eyes	94.7% [σ: 9.24 (3)]	89.3% [σ: 18.48 (3)]	16.5% [σ: 1.04 (17)]
Nose	100.0% [σ: 0.00 (2)]	50.0% [σ: 70.71 (2)]	3.5% [σ: 0.34 (17)]
HEAD SCAN 334			
	Spikes		1mm Accuracy
	Identified	Corrected	Other Points Moved
Entire Head	99.9% [σ: 0.48 (17)]	95.1% [σ: 6.86 (17)]	1.5% [σ: 0.14 (17)]
Back of Head	99.8% [σ: 0.73 (17)]	96.4% [σ: 6.31 (17)]	0.0% [σ: 0.00 (17)]
Ears	100.0% [σ: 0.00 (5)]	82.7% [σ: 28.91 (5)]	21.5% [σ: 2.16 (17)]
Eyes	100.0% [σ: 0.00 (3)]	100.0% [σ: 0.00 (3)]	7.2% [σ: 0.62 (17)]
Nose	100.0% [σ: 0.00 (1)]	100.0% [σ: 0.00 (1)]	2.9% [σ: 0.29 (17)]
HEAD SCAN 356			
	Spikes		1mm Accuracy
	Identified	Corrected	Other Points Moved
Entire Head	99.2% [σ: 1.24 (17)]	86.1% [σ: 14.03 (17)]	2.2% [σ: 0.33 (17)]
Back of Head	98.8% [σ: 1.98 (17)]	85.4% [σ: 17.99 (17)]	0.1% [σ: 0.01 (17)]
Ears	100.0% [σ: 0.00 (3)]	75.0% [σ: 25.00 (3)]	15.5% [σ: 1.61 (17)]
Eyes	100.0% [σ: 0.00 (2)]	100.0% [σ: 0.00 (2)]	7.5% [σ: 0.72 (17)]
Nose	100.0% [σ: 0.00 (3)]	95.2% [σ: 8.25 (3)]	7.0% [σ: 0.71 (17)]
HEAD SCAN DAN1			
	Spikes		1mm Accuracy
	Identified	Corrected	Other Points Moved
Entire Head	99.3% [σ: 1.50 (17)]	88.4% [σ: 14.36 (17)]	0.6% [σ: 0.07 (17)]
Back of Head	99.5% [σ: 1.07 (17)]	90.0% [σ: 13.99 (17)]	0.0% [σ: 0.00 (17)]
Ears	97.7% [σ: 7.54 (11)]	80.3% [σ: 35.60 (11)]	11.0% [σ: 1.36 (17)]
Eyes	100.0% [σ: 0.00 (3)]	100.0% [σ: 0.00 (3)]	6.1% [σ: 0.38 (17)]
Nose	100.0% [σ: 0.00 (1)]	100.0% [σ: 0.00 (1)]	2.4% [σ: 0.12 (17)]

TABLE B-6.
OPERATION: OPENING OF SIZE 4.0

HEAD SCAN 105			
	Spikes		1mm Accuracy
	Identified	Corrected	Other Points Moved
Entire Head	99.8% [σ: 0.61 (17)]	95.1% [σ: 6.86 (17)]	2.3% [σ: 0.00 (17)]
Back of Head	99.8% [σ: 0.67 (17)]	95.2% [σ: 7.50 (17)]	0.4% [σ: 0.01 (17)]
Ears	100.0% [σ: 0.00 (4)]	100.0% [σ: 0.00 (4)]	21.3% [σ: 0.00 (17)]
Eyes	100.0% [σ: 0.00 (2)]	93.8% [σ: 8.84 (2)]	2.3% [σ: 0.11 (17)]
Nose	100.0% [σ: 0.00 (1)]	100.0% [σ: 0.00 (1)]	2.7% [σ: 0.00 (17)]
HEAD SCAN 177			
	Spikes		1mm Accuracy
	Identified	Corrected	Other Points Moved
Entire Head	99.5% [σ: 1.07 (17)]	91.9% [σ: 6.51 (17)]	4.0% [σ: 0.02 (17)]
Back of Head	99.5% [σ: 1.37 (17)]	91.0% [σ: 7.57 (17)]	4.1% [σ: 0.03 (17)]
Ears	100.0% [σ: 0.00 (4)]	62.5% [σ: 47.87 (4)]	26.6% [σ: 0.01 (17)]
Eyes	92.0% [σ: 13.86 (3)]	82.7% [σ: 30.02 (3)]	19.2% [σ: 0.34 (17)]
Nose	100.0% [σ: 0.00 (2)]	50.0% [σ: 70.71 (2)]	4.7% [σ: 0.02 (17)]
HEAD SCAN 334			
	Spikes		1mm Accuracy
	Identified	Corrected	Other Points Moved
Entire Head	99.9% [σ: 0.48 (17)]	97.1% [σ: 4.57 (17)]	1.9% [σ: 0.00 (17)]
Back of Head	99.8% [σ: 0.73 (17)]	98.0% [σ: 4.33 (17)]	0.0% [σ: 0.00 (17)]
Ears	100.0% [σ: 0.00 (5)]	82.7% [σ: 28.91 (5)]	26.4% [σ: 0.03 (17)]
Eyes	100.0% [σ: 0.00 (3)]	100.0% [σ: 0.00 (3)]	9.2% [σ: 0.00 (17)]
Nose	100.0% [σ: 0.00 (1)]	100.0% [σ: 0.00 (1)]	2.5% [σ: 0.00 (17)]
HEAD SCAN 356			
	Spikes		1mm Accuracy
	Identified	Corrected	Other Points Moved
Entire Head	99.8% [σ: 0.52 (17)]	88.9% [σ: 11.77 (17)]	2.7% [σ: 0.03 (17)]
Back of Head	99.7% [σ: 0.75 (17)]	89.7% [σ: 14.75 (17)]	0.1% [σ: 0.00 (17)]
Ears	100.0% [σ: 0.00 (3)]	75.0% [σ: 25.00 (3)]	18.0% [σ: 0.02 (17)]
Eyes	100.0% [σ: 0.00 (2)]	100.0% [σ: 0.00 (2)]	8.2% [σ: 0.00 (17)]
Nose	100.0% [σ: 0.00 (3)]	95.2% [σ: 8.25 (3)]	8.7% [σ: 0.00 (17)]
HEAD SCAN DAN1			
	Spikes		1mm Accuracy
	Identified	Corrected	Other Points Moved
Entire Head	99.7% [σ: 0.95 (17)]	92.8% [σ: 10.41 (17)]	1.1% [σ: 0.00 (17)]
Back of Head	99.8% [σ: 0.81 (17)]	95.1% [σ: 8.61 (17)]	0.0% [σ: 0.00 (17)]
Ears	100.0% [σ: 0.00 (11)]	84.1% [σ: 35.83 (11)]	21.8% [σ: 0.03 (17)]
Eyes	100.0% [σ: 0.00 (3)]	100.0% [σ: 0.00 (3)]	7.1% [σ: 0.00 (17)]
Nose	100.0% [σ: 0.00 (1)]	100.0% [σ: 0.00 (1)]	2.4% [σ: 0.00 (17)]

TABLE B-7.
OPERATION: OPENING OF SIZE 4.5

HEAD SCAN 105			
	Spikes		1mm Accuracy
	Identified	Corrected	Other Points Moved
Entire Head	99.8% [σ: 0.53 (17)]	96.5% [σ: 5.21 (17)]	2.6% [σ: 0.01 (17)]
Back of Head	99.8% [σ: 0.67 (17)]	97.0% [σ: 5.50 (17)]	0.5% [σ: 0.01 (17)]
Ears	100.0% [σ: 0.00 (4)]	100.0% [σ: 0.00 (4)]	24.9% [σ: 0.00 (17)]
Eyes	100.0% [σ: 0.00 (2)]	78.6% [σ: 16.94 (2)]	3.2% [σ: 0.12 (17)]
Nose	100.0% [σ: 0.00 (1)]	100.0% [σ: 0.00 (1)]	5.1% [σ: 0.00 (17)]
HEAD SCAN 177			
	Spikes		1mm Accuracy
	Identified	Corrected	Other Points Moved
Entire Head	99.6% [σ: 1.06 (17)]	93.6% [σ: 4.11 (17)]	4.5% [σ: 0.02 (17)]
Back of Head	99.5% [σ: 1.36 (17)]	92.8% [σ: 4.90 (17)]	4.7% [σ: 0.03 (17)]
Ears	100.0% [σ: 0.00 (4)]	62.5% [σ: 47.87 (4)]	30.5% [σ: 0.01 (17)]
Eyes	93.3% [σ: 11.55 (3)]	85.3% [σ: 25.40 (3)]	21.4% [σ: 0.34 (17)]
Nose	100.0% [σ: 0.00 (2)]	50.0% [σ: 70.71 (2)]	6.4% [σ: 0.02 (17)]
HEAD SCAN 334			
	Spikes		1mm Accuracy
	Identified	Corrected	Other Points Moved
Entire Head	99.9% [σ: 0.48 (17)]	98.7% [σ: 2.13 (17)]	2.3% [σ: 0.00 (17)]
Back of Head	99.8% [σ: 0.73 (17)]	99.1% [σ: 2.16 (17)]	0.0% [σ: 0.00 (17)]
Ears	100.0% [σ: 0.00 (5)]	82.7% [σ: 28.91 (5)]	30.7% [σ: 0.03 (17)]
Eyes	100.0% [σ: 0.00 (3)]	100.0% [σ: 0.00 (3)]	11.4% [σ: 0.00 (17)]
Nose	100.0% [σ: 0.00 (1)]	100.0% [σ: 0.00 (1)]	3.3% [σ: 0.00 (17)]
HEAD SCAN 356			
	Spikes		1mm Accuracy
	Identified	Corrected	Other Points Moved
Entire Head	99.9% [σ: 0.48 (17)]	90.6% [σ: 10.85 (17)]	3.0% [σ: 0.03 (17)]
Back of Head	99.8% [σ: 0.69 (17)]	91.8% [σ: 13.08 (17)]	0.2% [σ: 0.00 (17)]
Ears	100.0% [σ: 0.00 (3)]	58.3% [σ: 52.04 (3)]	20.7% [σ: 0.02 (17)]
Eyes	100.0% [σ: 0.00 (2)]	100.0% [σ: 0.00 (2)]	8.5% [σ: 0.00 (17)]
Nose	100.0% [σ: 0.00 (3)]	95.2% [σ: 8.25 (3)]	11.1% [σ: 0.03 (17)]
HEAD SCAN DAN1			
	Spikes		1mm Accuracy
	Identified	Corrected	Other Points Moved
Entire Head	99.8% [σ: 0.55 (17)]	95.8% [σ: 7.13 (17)]	1.5% [σ: 0.00 (17)]
Back of Head	99.8% [σ: 0.81 (17)]	97.4% [σ: 5.81 (17)]	0.0% [σ: 0.00 (17)]
Ears	97.7% [σ: 7.54 (11)]	83.1% [σ: 31.78 (11)]	28.8% [σ: 0.02 (17)]
Eyes	100.0% [σ: 0.00 (3)]	100.0% [σ: 0.00 (3)]	8.4% [σ: 0.02 (17)]
Nose	100.0% [σ: 0.00 (1)]	100.0% [σ: 0.00 (1)]	5.3% [σ: 0.00 (17)]

TABLE B-8.
OPERATION: MEDIAN FILTER

HEAD SCAN 105			
	Spikes		2 Pixels
	Identified	Corrected	Other Points Moved
Entire Head	83.2% [σ: 17.77 (17)]	58.1% [σ: 33.00 (17)]	1.2% [σ: 0.10 (17)]
Back of Head	86.1% [σ: 15.05 (17)]	60.5% [σ: 33.96 (17)]	0.2% [σ: 0.18 (17)]
Ears	100.0% [σ: 0.00 (4)]	100.0% [σ: 0.00 (4)]	7.0% [σ: 0.01 (17)]
Eyes	98.4% [σ: 2.21 (2)]	89.1% [σ: 15.47 (2)]	3.9% [σ: 0.09 (17)]
Nose	100.0% [σ: 0.00 (1)]	100.0% [σ: 0.00 (1)]	6.5% [σ: 0.00 (17)]
HEAD SCAN 177			
	Spikes		2 Pixels
	Identified	Corrected	Other Points Moved
Entire Head	83.5% [σ: 17.00 (17)]	53.8% [σ: 30.74 (17)]	3.0% [σ: 0.12 (17)]
Back of Head	86.6% [σ: 13.24 (17)]	54.3% [σ: 30.62 (17)]	3.2% [σ: 0.23 (17)]
Ears	100.0% [σ: 0.00 (4)]	75.0% [σ: 28.87 (4)]	13.0% [σ: 0.00 (17)]
Eyes	98.7% [σ: 2.31 (3)]	90.7% [σ: 16.17 (3)]	19.5% [σ: 0.22 (17)]
Nose	100.0% [σ: 0.00 (2)]	100.0% [σ: 0.00 (2)]	9.3% [σ: 0.04 (17)]
HEAD SCAN 334			
	Spikes		2 Pixels
	Identified	Corrected	Other Points Moved
Entire Head	85.8% [σ: 14.95 (17)]	54.1% [σ: 33.36 (17)]	1.6% [σ: 0.16 (17)]
Back of Head	88.6% [σ: 12.58 (17)]	58.9% [σ: 32.60 (17)]	0.8% [σ: 0.20 (17)]
Ears	100.0% [σ: 0.00 (3)]	91.7% [σ: 14.43 (3)]	4.7% [σ: 0.01 (17)]
Eyes	100.0% [σ: 0.00 (2)]	100.0% [σ: 0.00 (2)]	9.5% [σ: 0.03 (17)]
Nose	95.2% [σ: 8.25 (3)]	76.2% [σ: 41.24 (3)]	15.6% [σ: 0.16 (17)]
HEAD SCAN 356			
	Spikes		2 Pixels
	Identified	Corrected	Other Points Moved
Entire Head	82.2% [σ: 17.30 (17)]	60.6% [σ: 31.47 (17)]	0.7% [σ: 0.06 (17)]
Back of Head	86.6% [σ: 14.81 (17)]	65.2% [σ: 31.21 (17)]	0.1% [σ: 0.08 (17)]
Ears	100.0% [σ: 0.00 (11)]	78.3% [σ: 31.67 (11)]	9.0% [σ: 0.07 (17)]
Eyes	100.0% [σ: 0.00 (3)]	100.0% [σ: 0.00 (3)]	10.9% [σ: 0.08 (17)]
Nose	100.0% [σ: 0.00 (1)]	100.0% [σ: 0.00 (1)]	8.4% [σ: 0.00 (17)]
HEAD SCAN DAN1			
	Spikes		2 Pixels
	Identified	Corrected	Other Points Moved
Entire Head	82.9% [σ: 18.55 (17)]	59.6% [σ: 32.25 (17)]	1.1% [σ: 0.08 (17)]
Back of Head	86.3% [σ: 14.40 (17)]	63.6% [σ: 32.60 (17)]	0.1% [σ: 0.14 (17)]
Ears	92.0% [σ: 17.89 (5)]	85.3% [σ: 20.22 (5)]	8.4% [σ: 0.03 (17)]
Eyes	100.0% [σ: 0.00 (3)]	100.0% [σ: 0.00 (3)]	9.9% [σ: 0.04 (17)]
Nose	100.0% [σ: 0.00 (1)]	100.0% [σ: 0.00 (1)]	9.9% [σ: 0.05 (17)]

TABLE B-9.
OPERATION: MEDIAN FILTER

HEAD SCAN 105			
	Spikes		3 Pixels
	Identified	Corrected	Other Points Moved
Entire Head	89.6% [σ: 12.39 (17)]	62.2% [σ: 33.38 (17)]	2.8% [σ: 0.15 (17)]
Back of Head	92.0% [σ: 9.33 (17)]	65.2% [σ: 34.73 (17)]	1.3% [σ: 0.26 (17)]
Ears	100.0% [σ: 0.00 (4)]	100.0% [σ: 0.00 (4)]	15.2% [σ: 0.01 (17)]
Eyes	98.4% [σ: 2.21 (2)]	93.8% [σ: 8.84 (2)]	8.4% [σ: 0.14 (17)]
Nose	100.0% [σ: 0.00 (1)]	100.0% [σ: 0.00 (1)]	16.1% [σ: 0.00 (17)]
HEAD SCAN 177			
	Spikes		3 Pixels
	Identified	Corrected	Other Points Moved
Entire Head	89.9% [σ: 12.54 (17)]	58.3% [σ: 32.49 (17)]	4.6% [σ: 0.17 (17)]
Back of Head	92.4% [σ: 8.38 (17)]	58.8% [σ: 32.89 (17)]	4.6% [σ: 0.33 (17)]
Ears	100.0% [σ: 0.00 (4)]	75.0% [σ: 28.87 (4)]	21.8% [σ: 0.01 (17)]
Eyes	97.3% [σ: 4.62 (3)]	88.0% [σ: 20.78 (3)]	28.2% [σ: 0.54 (17)]
Nose	100.0% [σ: 0.00 (2)]	100.0% [σ: 0.00 (2)]	18.2% [σ: 0.02 (17)]
HEAD SCAN 334			
	Spikes		3 Pixels
	Identified	Corrected	Other Points Moved
Entire Head	92.3% [σ: 9.14 (17)]	59.1% [σ: 35.47 (17)]	3.7% [σ: 0.23 (17)]
Back of Head	94.5% [σ: 6.95 (17)]	64.5% [σ: 33.97 (17)]	2.4% [σ: 0.28 (17)]
Ears	100.0% [σ: 0.00 (3)]	91.7% [σ: 14.43 (3)]	13.5% [σ: 0.01 (17)]
Eyes	100.0% [σ: 0.00 (2)]	100.0% [σ: 0.00 (2)]	14.2% [σ: 0.08 (17)]
Nose	95.2% [σ: 8.25 (3)]	76.2% [σ: 41.24 (3)]	26.4% [σ: 0.05 (17)]
HEAD SCAN 356			
	Spikes		3 Pixels
	Identified	Corrected	Other Points Moved
Entire Head	89.1% [σ: 12.16 (17)]	64.9% [σ: 32.05 (17)]	1.4% [σ: 0.09 (17)]
Back of Head	93.0% [σ: 9.17 (17)]	69.7% [σ: 32.12 (17)]	0.2% [σ: 0.15 (17)]
Ears	100.0% [σ: 0.00 (11)]	66.4% [σ: 34.97 (11)]	17.9% [σ: 0.06 (17)]
Eyes	100.0% [σ: 0.00 (3)]	100.0% [σ: 0.00 (3)]	15.9% [σ: 0.05 (17)]
Nose	100.0% [σ: 0.00 (1)]	100.0% [σ: 0.00 (1)]	21.0% [σ: 0.02 (17)]
HEAD SCAN DAN1			
	Spikes		3 Pixels
	Identified	Corrected	Other Points Moved
Entire Head	89.8% [σ: 13.12 (17)]	63.1% [σ: 33.10 (17)]	2.5% [σ: 0.12 (17)]
Back of Head	93.2% [σ: 8.65 (17)]	68.2% [σ: 33.86 (17)]	0.9% [σ: 0.23 (17)]
Ears	88.0% [σ: 26.83 (5)]	54.7% [σ: 44.07 (5)]	17.9% [σ: 0.05 (17)]
Eyes	98.5% [σ: 2.63 (3)]	100.0% [σ: 0.00 (3)]	16.5% [σ: 0.02 (17)]
Nose	100.0% [σ: 0.00 (1)]	0.0% [σ: 0.00 (1)]	18.6% [σ: 0.10 (17)]

TABLE B-10.
OPERATION: MEDIAN FILTER

HEAD SCAN 105	Spikes		4 Pixels
	Identified	Corrected	Other Points Moved
Entire Head	95.4% [σ: 6.51 (17)]	66.9% [σ: 32.96 (17)]	5.9% [σ: 0.24 (17)]
Back of Head	96.9% [σ: 4.19 (17)]	69.0% [σ: 33.46 (17)]	2.9% [σ: 0.45 (17)]
Ears	100.0% [σ: 0.00 (4)]	96.4% [σ: 7.14 (4)]	31.7% [σ: 0.03 (17)]
Eyes	96.9% [σ: 4.42 (2)]	90.6% [σ: 13.26 (2)]	19.2% [σ: 0.07 (17)]
Nose	100.0% [σ: 0.00 (1)]	0.0% [σ: 0.00 (1)]	39.4% [σ: 0.02 (17)]

HEAD SCAN 177	Spikes		4 Pixels
	Identified	Corrected	Other Points Moved
Entire Head	95.4% [σ: 6.96 (17)]	63.0% [σ: 32.88 (17)]	7.3% [σ: 0.27 (17)]
Back of Head	97.0% [σ: 2.99 (17)]	62.6% [σ: 32.67 (17)]	6.9% [σ: 0.54 (17)]
Ears	100.0% [σ: 0.00 (4)]	50.0% [σ: 40.82 (4)]	37.6% [σ: 0.01 (17)]
Eyes	57.3% [σ: 51.59 (3)]	37.3% [σ: 54.60 (3)]	46.2% [σ: 0.66 (17)]
Nose	100.0% [σ: 0.00 (2)]	100.0% [σ: 0.00 (2)]	37.3% [σ: 0.06 (17)]

HEAD SCAN 334	Spikes		4 Pixels
	Identified	Corrected	Other Points Moved
Entire Head	96.9% [σ: 5.05 (17)]	63.0% [σ: 35.48 (17)]	8.0% [σ: 0.25 (17)]
Back of Head	98.3% [σ: 2.83 (17)]	68.8% [σ: 32.99 (17)]	4.3% [σ: 0.43 (17)]
Ears	100.0% [σ: 0.00 (3)]	33.3% [σ: 28.87 (3)]	31.9% [σ: 0.02 (17)]
Eyes	100.0% [σ: 0.00 (2)]	100.0% [σ: 0.00 (2)]	22.4% [σ: 0.14 (17)]
Nose	95.2% [σ: 8.25 (3)]	42.9% [σ: 51.51 (3)]	42.7% [σ: 0.13 (17)]

HEAD SCAN 356	Spikes		4 Pixels
	Identified	Corrected	Other Points Moved
Entire Head	94.8% [σ: 6.99 (17)]	69.3% [σ: 30.72 (17)]	4.3% [σ: 0.17 (17)]
Back of Head	97.7% [σ: 3.71 (17)]	73.9% [σ: 31.67 (17)]	1.6% [σ: 0.33 (17)]
Ears	100.0% [σ: 0.00 (11)]	49.7% [σ: 41.73 (11)]	38.3% [σ: 0.12 (17)]
Eyes	100.0% [σ: 0.00 (3)]	50.0% [σ: 50.00 (3)]	30.2% [σ: 0.04 (17)]
Nose	100.0% [σ: 0.00 (1)]	50.0% [σ: 0.00 (1)]	43.4% [σ: 0.00 (17)]

HEAD SCAN DAN1	Spikes		4 Pixels
	Identified	Corrected	Other Points Moved
Entire Head	95.8% [σ: 7.03 (17)]	66.7% [σ: 32.94 (17)]	5.4% [σ: 0.22 (17)]
Back of Head	97.9% [σ: 3.61 (17)]	71.7% [σ: 33.80 (17)]	2.3% [σ: 0.44 (17)]
Ears	96.0% [σ: 8.94 (5)]	47.3% [σ: 48.67 (5)]	38.5% [σ: 0.04 (17)]
Eyes	98.5% [σ: 2.63 (3)]	81.8% [σ: 27.65 (3)]	26.1% [σ: 0.13 (17)]
Nose	100.0% [σ: 0.00 (1)]	0.0% [σ: 0.00 (1)]	44.8% [σ: 0.07 (17)]

TABLE B-11.
OPERATION: MEDIAN FILTER

HEAD SCAN 105			
	Spikes		5 Pixels
	Identified	Corrected	Other Points Moved
Entire Head	97.1% [σ: 4.56 (17)]	67.9% [σ: 32.41 (17)]	7.9% [σ: 0.30 (17)]
Back of Head	98.0% [σ: 3.18 (17)]	70.0% [σ: 32.42 (17)]	4.1% [σ: 0.57 (17)]
Ears	100.0% [σ: 0.00 (4)]	64.3% [σ: 47.38 (4)]	41.2% [σ: 0.04 (17)]
Eyes	96.9% [σ: 4.42 (2)]	82.8% [σ: 24.31 (2)]	26.1% [σ: 0.32 (17)]
Nose	100.0% [σ: 0.00 (1)]	0.0% [σ: 0.00 (1)]	51.3% [σ: 0.02 (17)]

HEAD SCAN 177			
	Spikes		5 Pixels
	Identified	Corrected	Other Points Moved
Entire Head	97.4% [σ: 4.15 (17)]	63.9% [σ: 31.16 (17)]	9.4% [σ: 0.32 (17)]
Back of Head	98.3% [σ: 1.65 (17)]	63.1% [σ: 30.68 (17)]	8.7% [σ: 0.61 (17)]
Ears	100.0% [σ: 0.00 (4)]	12.5% [σ: 25.00 (4)]	45.7% [σ: 0.01 (17)]
Eyes	53.3% [σ: 50.33 (3)]	1.3% [σ: 2.31 (3)]	53.9% [σ: 0.66 (17)]
Nose	100.0% [σ: 0.00 (2)]	50.0% [σ: 70.71 (2)]	50.5% [σ: 0.16 (17)]

HEAD SCAN 334			
	Spikes		5 Pixels
	Identified	Corrected	Other Points Moved
Entire Head	97.7% [σ: 4.51 (17)]	68.7% [σ: 32.83 (17)]	7.1% [σ: 0.29 (17)]
Back of Head	99.0% [σ: 1.65 (17)]	73.6% [σ: 33.48 (17)]	3.1% [σ: 0.60 (17)]
Ears	72.0% [σ: 43.82 (5)]	26.7% [σ: 43.46 (5)]	48.3% [σ: 0.04 (17)]
Eyes	98.5% [σ: 2.63 (3)]	80.3% [σ: 26.63 (3)]	31.7% [σ: 0.14 (17)]
Nose	100.0% [σ: 0.00 (1)]	0.0% [σ: 0.00 (1)]	57.5% [σ: 0.12 (17)]

HEAD SCAN 356			
	Spikes		5 Pixels
	Identified	Corrected	Other Points Moved
Entire Head	98.0% [σ: 4.10 (17)]	64.4% [σ: 34.40 (17)]	10.1% [σ: 0.32 (17)]
Back of Head	99.3% [σ: 1.02 (17)]	70.3% [σ: 30.98 (17)]	6.0% [σ: 0.51 (17)]
Ears	100.0% [σ: 0.00 (3)]	16.7% [σ: 28.87 (3)]	39.9% [σ: 0.03 (17)]
Eyes	100.0% [σ: 0.00 (2)]	83.3% [σ: 23.57 (2)]	32.1% [σ: 0.11 (17)]
Nose	61.9% [σ: 54.08 (3)]	42.9% [σ: 51.51 (3)]	52.7% [σ: 0.07 (17)]

HEAD SCAN DAN1			
	Spikes		5 Pixels
	Identified	Corrected	Other Points Moved
Entire Head	97.0% [σ: 4.82 (17)]	72.2% [σ: 29.84 (17)]	5.9% [σ: 0.21 (17)]
Back of Head	99.4% [σ: 1.13 (17)]	76.1% [σ: 31.37 (17)]	2.2% [σ: 0.45 (17)]
Ears	100.0% [σ: 0.00 (11)]	50.8% [σ: 42.89 (11)]	50.6% [σ: 0.07 (17)]
Eyes	91.7% [σ: 14.43 (3)]	50.0% [σ: 50.00 (3)]	38.3% [σ: 0.13 (17)]
Nose	100.0% [σ: 0.00 (1)]	0.0% [σ: 0.00 (1)]	53.8% [σ: 0.02 (17)]

TABLE B-12.
OPERATION: MEDIAN FILTER

HEAD SCAN 105			
	Spikes		6 Pixels
	Identified	Corrected	Other Points Moved
Entire Head	97.9% [σ: 3.19 (17)]	68.7% [σ: 30.91 (17)]	10.2% [σ: 0.39 (17)]
Back of Head	98.4% [σ: 2.57 (17)]	70.8% [σ: 31.20 (17)]	5.8% [σ: 0.73 (17)]
Ears	100.0% [σ: 0.00 (4)]	64.3% [σ: 47.38 (4)]	50.3% [σ: 0.06 (17)]
Eyes	96.9% [σ: 4.42 (2)]	75.0% [σ: 35.36 (2)]	33.8% [σ: 0.42 (17)]
Nose	100.0% [σ: 0.00 (1)]	0.0% [σ: 0.00 (1)]	59.9% [σ: 0.02 (17)]
HEAD SCAN 177			
	Spikes		6 Pixels
	Identified	Corrected	Other Points Moved
Entire Head	98.3% [σ: 2.40 (17)]	65.1% [σ: 29.55 (17)]	11.8% [σ: 0.41 (17)]
Back of Head	98.7% [σ: 1.26 (17)]	63.6% [σ: 28.30 (17)]	10.7% [σ: 0.74 (17)]
Ears	100.0% [σ: 0.00 (4)]	12.5% [σ: 25.00 (4)]	53.6% [σ: 0.04 (17)]
Eyes	60.0% [σ: 52.92 (3)]	0.0% [σ: 0.00 (3)]	60.2% [σ: 0.58 (17)]
Nose	100.0% [σ: 0.00 (2)]	50.0% [σ: 70.71 (2)]	61.7% [σ: 0.02 (17)]
HEAD SCAN 334			
	Spikes		6 Pixels
	Identified	Corrected	Other Points Moved
Entire Head	98.4% [σ: 2.95 (17)]	71.6% [σ: 33.72 (17)]	9.6% [σ: 0.40 (17)]
Back of Head	99.3% [σ: 1.26 (17)]	76.3% [σ: 33.59 (17)]	4.7% [σ: 0.84 (17)]
Ears	100.0% [σ: 0.00 (5)]	23.3% [σ: 43.46 (5)]	55.9% [σ: 0.06 (17)]
Eyes	97.0% [σ: 5.25 (3)]	43.9% [σ: 41.25 (3)]	41.7% [σ: 0.20 (17)]
Nose	100.0% [σ: 0.00 (1)]	0.0% [σ: 0.00 (1)]	67.4% [σ: 0.02 (17)]
HEAD SCAN 356			
	Spikes		6 Pixels
	Identified	Corrected	Other Points Moved
Entire Head	98.5% [σ: 2.79 (17)]	64.7% [σ: 33.45 (17)]	12.8% [σ: 0.41 (17)]
Back of Head	99.2% [σ: 1.44 (17)]	71.3% [σ: 29.81 (17)]	8.2% [σ: 0.62 (17)]
Ears	100.0% [σ: 0.00 (3)]	16.7% [σ: 28.87 (3)]	47.9% [σ: 0.05 (17)]
Eyes	50.0% [σ: 70.71 (2)]	33.3% [σ: 47.14 (2)]	41.4% [σ: 0.11 (17)]
Nose	90.5% [σ: 16.49 (3)]	38.1% [σ: 54.08 (3)]	60.0% [σ: 0.10 (17)]
HEAD SCAN DAN1			
	Spikes		6 Pixels
	Identified	Corrected	Other Points Moved
Entire Head	97.9% [σ: 3.30 (17)]	74.8% [σ: 29.31 (17)]	8.3% [σ: 0.28 (17)]
Back of Head	99.7% [σ: 0.89 (17)]	77.8% [σ: 31.38 (17)]	3.9% [σ: 0.61 (17)]
Ears	100.0% [σ: 0.00 (11)]	55.3% [σ: 39.49 (11)]	61.2% [σ: 0.06 (17)]
Eyes	58.3% [σ: 52.04 (3)]	41.7% [σ: 38.19 (3)]	48.4% [σ: 0.06 (17)]
Nose	100.0% [σ: 0.00 (1)]	0.0% [σ: 0.00 (1)]	61.3% [σ: 0.02 (17)]

U. S. Government Printing Office 1995 750-071/00141